Check for updates

*Advanced Healthcare Materials*

ADVANCED HEALTHCARE MATERIALS
www.advhealthmat.de

RESEARCH ARTICLE OPEN ACCESS

# Nanobiosensor Based on Catalytic Palladium Nanoclusters and Oxidases for Bianalyte Electrochemical Determination: Glucose and Ethanol in Sweat

Alejandro Rodríguez-Penedo[1,2] | Estefanía Costa-Rama[1,2] | Beatriz Fernández[1,2] | M. Teresa Fernández-Abedul[1,2]

[1]Department of Physical and Analytical Chemistry, University of Oviedo, Oviedo, Spain | [2]Biomedical Engineering Center, University of Oviedo, Oviedo, Spain

**Correspondence:** Estefanía Costa-Rama (costaestefania@uniovi.es) | M. Teresa Fernández-Abedul (mtfernandeza@uniovi.es)

**Received:** 4 September 2025 | **Revised:** 27 January 2026 | **Accepted:** 4 February 2026

**Keywords:** electrochemical biosensors | ethanol | glucose | nanoclusters | sweat analysis

## ABSTRACT

Monitoring metabolites through non-invasive methods is revolutionizing clinical analysis, with decentralized and faster tests. Sweat, a readily available biological fluid that requires non-invasive and simple procedures, is emerging as a valuable source of key biomarkers, such as glucose and ethanol. In this work, an enzymatic nanobiosensor for simultaneous determination of glucose and ethanol in sweat samples has been developed. The electrochemical platform consists of two working electrodes onto which Pd nanoclusters (PdNCs) with catalytic activity for the oxygen reduction reaction were deposited. Additionally, each WE was modified either with glucose oxidase (GOx) or alcohol oxidase (AOx). Thus, the simultaneous quantification of both analytes, glucose and ethanol, was performed thanks to the localized decrease in the concentration of dissolved $O_2$ produced at each WE by the oxidase enzymes. This resulted in a reduction of the current density measured by cyclic voltammetry. Sweat samples were collected using a polyamide membrane that permits extremely rapid analysis without the need for any external solution or sample pretreatment, making the method user-friendly and well-suited for self-analysis. The results revealed the capability of the nanobiosensor for determining the increase in the level of both analytes in sweat after the consumption of alcoholic beverages and energy drinks.

## 1 | Introduction

The use of biosensors to monitor metabolites in biological fluids through non-invasive methods marks a significant breakthrough, greatly enhancing the simplicity and accessibility of analyses while enabling their decentralization, being the future of clinical analysis [1, 2]. Among all the biological components, enzymes continue receiving tremendous interest, being highly selective and requiring procedures with minimal steps, usually performed at easily achievable conditions (mild pH values and temperatures). Regarding the transduction component of biosensors, electrochemical systems stand out because they combine basic properties as sensitivity and precision with others such as affordability, ease of miniaturization and adaptability to point-of-care (POC) analysis, [3] including for example, wearable, portable or implantable systems [4]. Electrochemical transduction fits properly with oxidase or reductase enzymes since they catalyze redox reactions. From the first generation of oxidase-catalyzed based biosensors, that utilize dissolved oxygen as an electron acceptor [5], a second and third generations have arisen, adding redox mediators [6], or immobilizing directly the enzyme and nanomaterials on electrodes to improve their performance [7]. A fourth one based on replacing organic enzymes with catalytical artificial nanomaterials is under development [8]. Although the use of redox mediators eliminates the dependence on oxygen, its addition complicates the procedure. Combination of enzymes

This is an open access article under the terms of the Creative Commons Attribution-NonCommercial License, which permits use, distribution and reproduction in any medium, provided the original work is properly cited and is not used for commercial purposes.
© 2026 The Author(s). *Advanced Healthcare Materials* published by Wiley-VCH GmbH

with nanocatalysts acting on oxygen-based reactions could be a simple alternative with fast readout.

Nanomaterials are commonly combined with bioelectrochemical approaches, becoming popular with enzymatic biosensors, since they can favor the immobilization of enzymes and greatly improve the sensitivity and precision of the measurements, resulting in a significant reduction of the detection limits [9]. From the wide variety of nanomaterials, metallic nanoclusters (NCs) have gained significant popularity due to their simplicity of synthesis, stability, and broad range of applications [10, 11]. When NCs are synthesized using thiolate protective ligands, they exhibit uniform size, are soluble in aqueous media, and possess remarkable stability, which is further enhanced when bidentate ligands are employed [12]. It has been demonstrated that palladium nanoclusters (PdNCs) exhibit intense catalytic activity on both hydrogen evolution reaction (HER) [13] and oxygen reduction reaction (ORR) [14, 15], making them highly suitable for electrocatalytical analysis [16]. Moreover, Pd is one of the most efficient catalytic metals for the ORR. Although Pt still exhibits the highest catalytic activity over this reaction, its extremely low natural abundance, estimated to be nearly 50 times lower than Pd, reduces its applicability [17]. In contrast, Pd offers an attractive balance between catalytic performance, availability and cost. In addition, PdNCs have also been shown to be stable for at least 1 week when deposited on screen-printed electrodes (SPEs) [15], which makes them ideal as electrode modifiers. The use of SPE cards containing 2 (or more) working electrodes (WEs), allows: i) increasing the accuracy of the measurements by recording more than one simultaneously [13], ii) using one as control for monitoring non-specific signals [18] or, iii) performing multiplexed analysis when electrodes are modified with different recognition elements [19].

When developing devices for decentralized analysis is important to consider collecting samples with minimally invasive procedures. In this sense, sweat can be easily collected without needing a complicate treatment [20], ideal for skin-mounted devices to perform continuous measurement of key biomarkers [21]. Therefore, flexible electrochemical sensors are highly suitable for wearable sweat analysis due to their adaptability, lightness and small size [22], being particularly interesting those capable of simultaneous determination of multiple analytes [23].

Undoubtedly, glucose sensors stand out among the enzymatic electroanalytical biosensors, initially developed with glucose oxidase (GOx) as early as in the 1960s, and steadily evolved to the present day [24]. Glucose is the gold-standard for monitoring metabolic diseases as diabetes, estimated to cost approximately 760 billion dollars per year [25], but also has relevance in other fields. For example, it allows determination of the efficiency of energy metabolism as well as the effect on the athletic performance, not only during training [26], but also during recovery and sleep phases [27]. Sweat measurement is an alternative to frequent capillary puncture in diabetic patients [28]. and, also permits immediate analysis, providing real-time information without interrupting the athlete's physical activity. No need to say that this is especially important in athletes with diabetes [29].

Furthermore, alcohol consumption can trigger hypoglycemia by reducing glycogenesis [30], particularly relevant for people with diabetes [31]. In addition, continued alcohol consumption can cause severe and prolonged hypoglycemia even in healthy individuals [32]. This effect is increased when alcoholic beverages are combined with simple carbohydrates, such as those contained in cocktails [32]. Therefore, the simultaneous measurement of glucose and ethanol in minimally invasive samples could advance the knowledge in this area [33]. In the case of glucose, the concentration in sweat is notably lower than that reported in blood, approximately 1% [21], although it has been proven that this correlation is quite altered due to factors such as diet or physical exercise [34]. On the other hand, the concentration of ethanol in sweat can be higher (approximately 20%) than that found in blood [35]. This makes sweat a valuable alternative to traditional blood or breath measurements that could provide useful information.

This work explores an approach different from conventional glucose biosensors, focusing on the use of PdNCs alongside oxidase enzymes immobilized on the WE. The key difference from third-generation sensors lies in the fact that PdNCs do not exchange electrons with the enzyme. Instead, their analytical signal, based on the electrocatalysis of the ORR, is influenced by changes in the localized oxygen concentration on the surface electrode, produced by immobilized oxidase enzymes. Therefore, as the concentration of analyte in the solution increases, there is a greater decrease in $O_2$, and consequently, immobilized PdNCs produce a decrease in the electrocatalytical signal. Thus, the developed nanobiosensor is a hybrid between first and third generations, combining bio and nanocatalysts for enhanced glucose and ethanol sensing.

## 2 | Experimental

### 2.1 | Materials and Reagents

For the synthesis of PdNCs, high-purity potassium tetrachloropalladate was used as the precursor salt, reduced DL-6,8-thioctic acid (DHLA) as the stabilizing agent, and sodium borohydride as the reducing agent, all provided by Sigma-Aldrich. Ultrapure water (Pure-lab Flex 3; ELGA-Veolia), with a resistivity of 18.2 MΩ cm, was used as the solvent, and the synthesis was carried out in basic medium using sodium hydroxide (Sigma-Aldrich). To purify the synthesized PdNCs, Amicon Ultra-0.5 filters (membrane PLBC, Millipore Amicon) with a 3 KDa cutoff were employed.

The enzymes utilized were GOx from *Aspergillus niger* and alcohol oxidase (AOx) from *Candida boidinii*, both from Sigma-Aldrich. For the bioconjugation of GOx with PdNCs, 1-ethyl-3-(3-dimethylaminopropyl) carbodiimide (EDC) (Across Organics) and N-hydroxysuccinimide (NHS) (Sigma-Aldrich) were used. The purification of bioconjugates was performed using Amicon Ultra-0.5 filters (membrane PLBC, Millipore Amicon) with a 100 KDa cutoff. Pure $O_2$ (> 99.995%) and $N_2$ (> 99.999%), both from Alphagaz, were also used.

Phosphate-buffered saline (PBS) pH 7.0 solution was prepared using disodium hydrogen phosphate anhydrous (VWR), sodium dihydrogen phosphate dihydrate (VWR), sodium chloride (Sigma-Aldrich), and potassium chloride (Sigma-Aldrich). The



21922659, 2026, 16, Downloaded from https://advanced.onlinelibrary.wiley.com/doi/10.1002/adhm.202504371 by Spanish Cochrane National Provision (Ministerio de Sanidad), Wiley Online Library on [27/04/2026]. See the Terms and Conditions (https://onlinelibrary.wiley.com/terms-and-conditions) on Wiley Online Library for rules of use; OA articles are governed by the applicable Creative Commons License

final concentrations were 10 mM for phosphate, 137 mM for sodium chloride and 2.7 mM for potassium chloride.

Sodium chloride, sodium dihydrogen phosphate dihydrate, and L-histidine (Sigma-Aldrich) were used to prepare artificial sweat. This was made according to the International Standard Organization (ISO105-E04-2008 E), solving 0.5 g of NaCl, 0.05 g of L-histidine and 0.5 g of $NaH_2PO_4$ in ultrapure water and bringing to a volume of 100 mL. The pH was adjusted to 7.0 to match that of the PBS used.

The solutions of GOx and AOx were prepared in PBS pH 7.0, while glucose and ethanol solutions were prepared in this buffer solution or in artificial sweat, depending on the study.

Woven cotton (from the inside of commercial plasters, Hartmann), membrane for screen-printed electrodes with an approximate area of 0.7 $cm^2$ (Metrohm Dropsens) and Anodisc alumina filter discs 0.2-μm pore size (Whatman) were evaluated to collect sweat, in all cases completely covering all the electrodes of the electrochemical cell. Adhesive film ARcare 90445Q was used for placing the SPE on the skin. Potassium hexacyanoferrate (III) and potassium hexacyanoferrate (II) trihydrate, both from Sigma-Aldrich were used to perform impedance measurements.

Flexible SPEs from MicruX Technologies (Spain) were employed. These included a carbon-ink counter electrode (CE), a silver-ink pseudoreference electrode (RE), and either a single circle-shaped WE with an area of 7.1 $mm^2$ (1WE-SPE), or two oval-shaped WEs (2WE-SPE) each measuring 2.3 $mm^2$ of area (in both cases WEs were made of carbon-ink).

## 2.2 | Instrumentation

For the characterization of the PdNCs, an absorbance spectrophotometer Multiskan Skyhigh (Thermo Scientific) with a quartz cuvette model 114F-QS (Sigma-Aldrich), a high-resolution transmission electron microscope (HR-TEM) model Libra 200 FE (Carl Zeiss), and an inductively coupled plasma mass spectrometry (ICP-MS) model 7900 (Agilent) were used.

Electrochemical measurements using single WE cards were carried out with a μ-Autolab Type II potentiostat (EcoChemie BV), while those made using cards with 2 WEs were made with a μStat 200 (Metrohm) bipotentiostat. A suitable box connector from MicruX Technologies was used as interface between the SPEs and the potentiostats. A USB-sized bipotentiostat (MicruX Technologies) connected to the smartphone was also used. Moreover, for Electrochemical Impedance Spectroscopy (EIS) studies, the potentiostat ECStat (MicruX Technologies) was used, with the *EIS analyzer* free software version 1.0 for data processing.

## 2.3 | Methods

### 2.3.1 | Synthesis of PdNCs

For the synthesis of PdNCs a previously developed protocol was used [15]. Figure 1A (left) shows a schematic of the synthesis protocol that can be summarized as follows: 0.0125 g of DHLA were added to 10 mL of ultrapure water containing 120 μL of 2 M NaOH; the mixture was stirred at 37 °C for 2 min and then, 500 μL of 15 mM $K_2PdCl_4$ was added dropwise and allowed to interact for 5 min; finally, 1 mL of 0.5 M $NaBH_4$ was added under vigorous stirring. After allowing the reaction to stabilize for 6 h, the synthesized PdNCs were purified by ultracentrifugation using 10 KDa membrane filters in 4 cycles of 10 min each at 5500 rpm, with ultrapure water washes between cycles. Final PdNCs dispersions were stored at room temperature (RT), protected from light, and they were characterized by absorbance spectroscopy, HR-TEM, and ICP-MS.

### 2.3.2 | Modification of Single and Dual SPEs

The modification of the SPEs with PdNCs was performed as follows. In the case of 1WE-SPEs, 6 μL of 4-μg $mL^{-1}$ PdNCs dispersion (in PBS) were deposited onto the WE and left to dry for 40 min at 37 °C. The same procedure was followed for 2WE-SPEs but using only 1.5 μL of the PdNCs dispersion. To modify the WE of the 1WE-SPEs with PdNCs and the enzymes, GOx or AOx, 6 μL of a mixture containing 4 μg $mL^{-1}$ of PdNCs and either 1667 U $mL^{-1}$ of GOx, or 83 U $mL^{-1}$ of AOx were used. In the case of 2WE-SPCE, 1.5 μL of a mixture containing 5.2 μg $mL^{-1}$ of PdNCs and either 2160 U $mL^{-1}$ of GOx, or 108 U $mL^{-1}$ of AOx were used instead.

### 2.3.3 | Electrochemical Measurements Using Single and Dual SPEs

To perform the electrochemical measurements, with either 1WE-SPEs or 2WE-SPEs, 50 μL of the working solution were placed on the screen-printed card covering all the electrodes. The cyclic voltammograms (CVs) were performed by scanning the potential between 0 and −1.2 V at a scan rate of 100 mV $s^{-1}$. All electrochemical measurements were performed at RT or at 37 °C using a new SPE for each measurement. To process the results, the current or current density values obtained at a potential of −0.55 V were used.

To increase the oxygen concentration of the solutions, $O_2$ was bubbled (at a flow rate of 20 mL $min^{-1}$) for a time comprised between 1.5 and 15 min. On the other hand, to decrease the dissolved oxygen, $N_2$ was bubbled (at 20 mL $min^{-1}$) for a time ranging between 1 and 7 min.

The EIS measurements were performed using the hexacyanoferrate (II)/(III) redox pair, both components with a concentration of 5 mM prepared in 10 mM PBS pH 7.0. A cyclic voltammogram was first performed to obtain the redox potential of the pair. Once obtained, the EIS scan was performed, sweeping between 0.1 and $10^6$ Hz, measuring a total of 70 frequencies.

### 2.3.4 | Collection and Measurement of Sweat Samples

To collect sweat samples, the volunteers washed their faces thoroughly, especially the forehead, with soap and water, then rinsed with water and dried completely with paper towels. Following this, they engaged in 30 min of moderate-intensity aerobic



21922659, 2026, 16, Downloaded from https://advanced.onlinelibrary.wiley.com/doi/10.1002/adhm.202504371 by Spanish Cochrane National Provision (Ministerio de Sanidad), Wiley Online Library on [27/04/2026]. See the Terms and Conditions (https://onlinelibrary.wiley.com/terms-and-conditions) on Wiley Online Library for rules of use; OA articles are governed by the applicable Creative Commons License

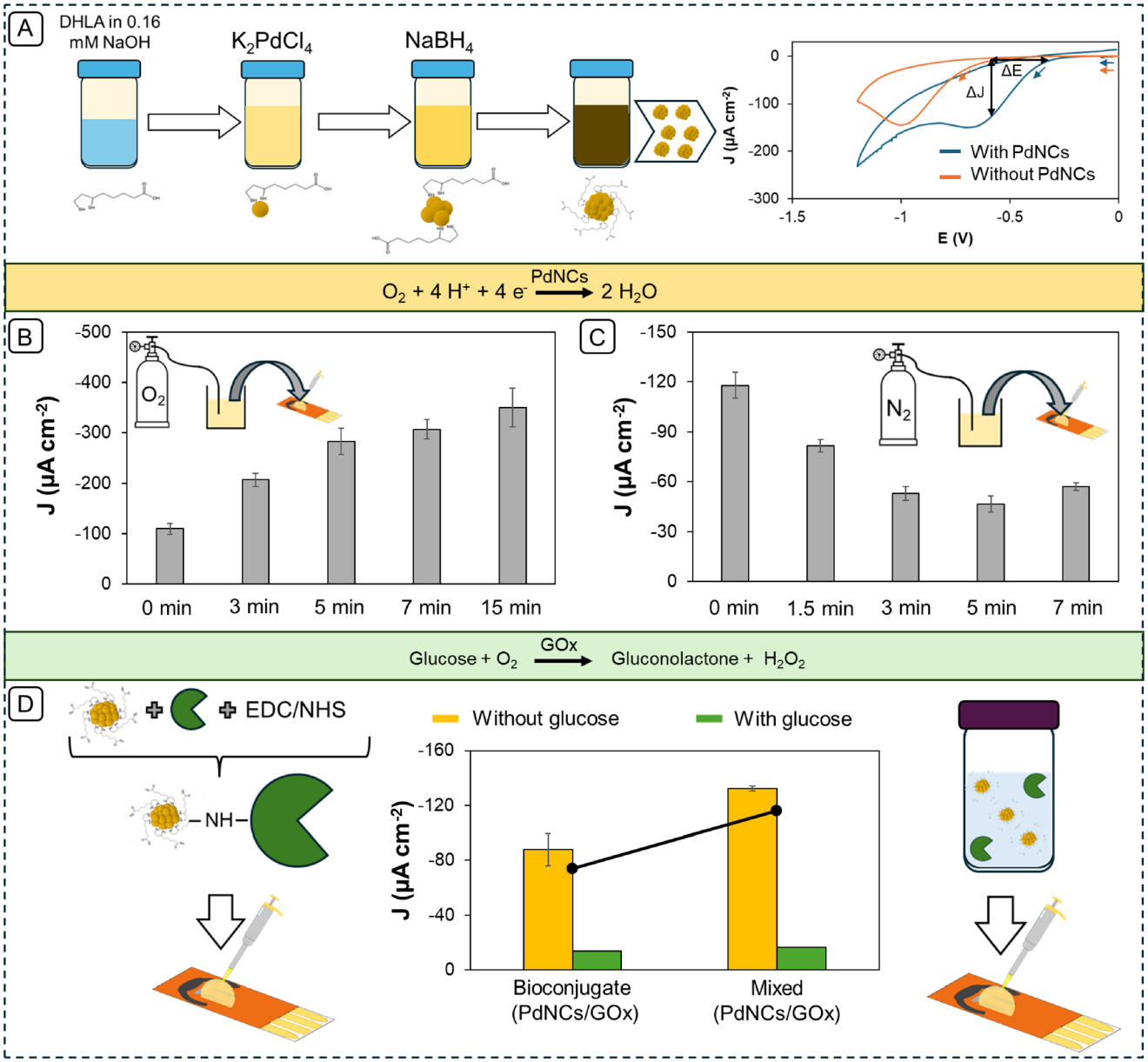



**FIGURE 1** | Synthesis of PdNCs and influence of $O_2$ concentration on ORR: (A) Diagram of the PdNCs synthesis protocol and comparison of electrochemical measurements in 10 mM PBS pH 7.0 using 1WE-SPEs unmodified (orange) and modified with 6 μL of PdNCs dispersion (4 μg mL$^{-1}$) (blue); (B,C) Current densities obtained with PdNCs-modified 1WE-SPE when CVs were recorded in PBS after bubbling $O_2$ (B) or $N_2$ (C) for different times. (D) Comparison of the current densities obtained for electrodes modified with 6 μL of 10 mM of PBS pH 7.0 containing 4 μg mL$^{-1}$ (i.e., 0.34 μg cm$^{-2}$) of PdNCs and 1667 U mL$^{-1}$ (i.e., 141 U cm$^{-2}$) of GOx being bioconjugated (left) or mixed (right), when using as buffer 10 mM of PBS (green). A blank was also recorded (yellow). The black dots show the ΔJ. Error bars show the standard deviation (SD) for measurements recorded in 3 SPEs.

exercise (alternating between running and walking). The outside temperature fluctuated between 8 and 15 °C, and none of the days were rainy or windy. Sweat samples were collected directly from the participants' foreheads using the selected absorbent material. When multiple consecutive experiments were necessary (e.g., consumption of sugary or alcoholic drinks), participants took a 15-min break to consume the respective beverages and wash and dry their faces as done previously.

To perform the measurements, the sweat-soaked absorbent was immediately placed onto the SPE cell previously nanobiomodified as indicated previously. A new electrochemical cell and sweat-soaked absorbent were used for each measurement.

A calibration curve with external standards, prepared using artificial sweat as solvent, was performed. For this calibration, polyamide membranes were placed over nanobiomodified 2WE-SPEs (each WE modified with GOx and AOx, respectively, apart from PdNCs), in order to simulate the measurement procedure for the samples. Then, 10 μL of the prepared standards containing either glucose or ethanol (or both) were deposited onto the polyamide membrane to perform the measurements.



21922659, 2026, 16, Downloaded from https://advanced.onlinelibrary.wiley.com/doi/10.1002/adhm.202504371 by Spanish Cochrane National Provision (Ministerio de Sanidad), Wiley Online Library on [27/04/2026]. See the Terms and Conditions (https://onlinelibrary.wiley.com/terms-and-conditions) on Wiley Online Library for rules of use; OA articles are governed by the applicable Creative Commons License

This protocol was explained in detail to the participants in the study, who voluntarily provided their informed written consent by signing the document included in the Supporting Information. Data confidentiality was ensured, in accordance with the Declaration of Helsinki on biomedical research involving human subjects. Since the number of participants was small and samples were collected through non-invasive procedures, it was not considered necessary to ask the Ethics Committee for approval. At no point were measurements taken directly on the skin or using wearable formats. Sweat samples were collected using polyamide membranes, which were placed on the SPEs to record measurements, to prevent PdNCs and enzymes from contacting the skin.

#### 2.3.5 | Statistical analysis

The results of this study are shown as the mean accompanied by the standard deviation, indicating the sample size (n) in each of the experiments performed. To find significant differences, Student's *t*-test for paired samples was used with a confidence level of 95%, ensuring that the variances were equal in both groups using the F-test. All statistical analyses were performed using Microsoft Excel (version 2601), except for the EIS measurements, which were processed using EIS analyzer free software (version 1.0).

## 3 | Results and Discussion

### 3.1 | Influence of Oxygen Present in the Solution

PdNCs synthesized using DHLA have demonstrated abundant catalytic activity on the ORR when working in neutral media [15], thus allowing the performance of electrochemical measurements without requiring additional steps of medium exchange for samples under physiological conditions. The catalytic effect of the synthesized PdNCs on the ORR can be observed in Figure 1A (right) where CVs recorded on 10 mM PBS pH 7.0 using unmodified and PdNCs-modified SPEs are compared. Although screen-printed electrodes could be reused, a regeneration treatment would increase analysis time, require qualified personnel as well as careful optimization to guarantee intra-electrode precision. Therefore, each measurement was recorded on a new SPE platform.

Regarding the medium employed for the measurements, 10 mM PBS pH 7.0 has a composition more similar to artificial sweat used in the calibration. Acetate buffer pH 5.6 was also tested, since this pH is closer to the optimum for GOx (5.5, with a working range comprised between 4.0 and 7.0) as specified by the company, and it is also adequate for AOx (with an optimum of 7.5, according to the provided data sheet), with a range between 5 and 9 [36]. However, not only the biocatalytical effect should be considered but also the electrocatalytic properties of the PdNCs. As can be seen in CVs of Figure S1, the current density is greatly reduced when acetate buffer is used, which may be due to the acidic pH that induces their aggregation. Thus, 10 mM PBS pH 7.0 was selected for all subsequent experiments.

Figure 1A also illustrates the two options to evaluate the change in the signal: the variation that occurs in the intensity (i, in μA) or current density (J, in μA $cm^{-2}$) at a fixed potential (E, in V), or the change in the potential at which a given current intensity or density is reached. In this work, the first option is preferred, as a decrease in the $O_2$ concentration of the solution significantly reduces the current density of the peak observed at ca. −0.55 V (in PdNCs-modified SPEs), leading to increased precision. The example shows the cyclic voltammograms for modified (with 6 μL containing 4 μg $mL^{-1}$ of PdNCs) and unmodified WEs, being the difference in current density at a potential of −0.55 V of −102 μA $cm^{-2}$ while the difference in the potential at which a current density of 100 μA $cm^{-2}$ is reached was −0.4 V. Also, measuring current density (at a given potential) instead of current intensity was chosen since WEs with different areas will be used along the work. Moreover, it was simpler to measure the signal directly instead of subtracting the signals from the blank to make the increment, so for the rest of the work direct measurements will be shown (intensities of current are measured from the baseline). Although there is also the possibility of measuring the potential at which a certain current density is reached, data processing is more complex and the bipotentiostat that will be used when working with a SPE cell with 2 WEs, only allows measurements to be taken every 0.005 V, which would result in a decrease in the precision of the measures.

The concentration of oxygen in solution is a crucial parameter since it will be the basis of the analysis. Thus, Figure 1B,C evaluate how the catalytic activity of the PdNCs is affected by the variation in the concentration of dissolved oxygen, by using external $O_2$ and $N_2$ flows. On the one hand, pure oxygen was bubbled (at 20 mL $min^{-1}$) in a tube containing 15 mL of PBS for different times (between 0 and 15 min), and then 50 μL of the solution was deposited onto a PdNCs-modified 1WE-SPE to record a CV. As can be seen in Figure 1B, a notable increase in the current density (measured at −0.55 V) occurred, starting with a current density of −110 ± 11 μA $cm^{-2}$, rising to −207 ± 13 μA $cm^{-2}$ in only 3 min of $O_2$ bubbling, and reaching −350 ± 40 μA $cm^{-2}$ when $O_2$ was bubbled for 15 min, resulting in an overall increase of 318%. There is not an appreciable increase beyond this time. On the other hand, Figure 1C shows the experimental results after bubbling pure $N_2$ (at 20 mL $min^{-1}$) for up to 7 min. In contrast to that observed in Figure 1B, the current density obtained significantly decreases as $N_2$ bubbling time increases, from −118 ± 8 to −47 ± 5 μA $cm^{-2}$ when $N_2$ flowed for 5 min. Thus, using oxygen-oversaturated solutions increases the analytical signal, which could be potentially applied to the improvement of the analytical performance when electrocatalytic activity of PdNCs on ORR was used in applications requiring higher sensitivity. In subsequent studies, bio and nanocatalysts were combined using glucose oxidase, apart from PdNCs. Thus, the enzymatic reaction decreases the concentration of oxygen, which in turn reduces the catalytic cathodic current due to the reduction of oxygen at the PdNCs-modified electrode (reactions in Figure 1).

Three different approaches were considered to combine both bio (oxidase enzyme) and nano (PdNCs) catalysts: (i) synthesis of PdNCs using an oxidase enzyme as ligand, (ii) bioconjugation of PdNCs with an oxidase enzyme, and (iii) mixing in solution PdNCs with the oxidase enzyme. Initially, the synthesis of PdNCs was modified by substituting DHLA by the enzyme, attempting



21922659, 2026, 16, Downloaded from https://advanced.onlinelibrary.wiley.com/doi/10.1002/adhm.202504371 by Spanish Cochrane National Provision (Ministerio de Sanidad), Wiley Online Library on [27/04/2026]. See the Terms and Conditions (https://onlinelibrary.wiley.com/terms-and-conditions) on Wiley Online Library for rules of use; OA articles are governed by the applicable Creative Commons License

to emulate the synthesis of NCs using proteins as followed by other authors [37]. However, no PdNCs (or other types of nanomaterials) with catalytic activity on ORR could be obtained. The next option was the bioconjugation of the enzyme with PdNCs using EDC-NHS chemistry to generate amide bonds as previously reported [38, 39]. This bioconjugate was then deposited onto the electrodes for measurement. The last option was to modify the WE with a mixture of enzyme and PdNCs dispersion, without adding any reagent for covalent bioconjugation. The results for the last two methods are collected in Figure 1D.

Initially, it was hypothesized that the closer PdNCs are to the enzyme, and so to the active center where oxygen decreases, as well as to the electrode surface, where the oxygen reduction happens, the more significant the decrease of the analytical signal will be, thus improving the sensitivity. However, as shown in Figure 1D, a signal of $-132 \pm 12$ μA cm$^{-2}$ was found for the electrode modified with the mixture of PdNCs and GOx, while only $-88 \pm 11$ μA cm$^{-2}$ was obtained for the case of the bioconjugation (i.e., 35% lower signal). Therefore, not only there was no improvement after bioconjugation, but also the current density was reduced, probably due to the loss of activity of certain enzyme molecules during bioconjugation or the loss of PdNCs or enzyme during the purification step.

### 3.2 | Optimization and Characterization of the Nanobiosensors Based on PdNCs

Once it was decided that the measurements would be performed by depositing a mixture containing the enzyme along with the PdNCs without using any bioconjugation method, nanobiosensors for glucose and, also, for ethanol (using AOx enzyme and the same approach as that for GOx) were prepared. The development of multianalyte methodologies is of paramount relevance. In this case, as oxygen participates as mediator in the enzymatic reactions catalyzed by oxidases, this versatile detection methodology can be applied to the determination of their respective substrates, combining both sensitivity with selectivity. First, independent sensors were employed, one for glucose and another for ethanol.

In both cases, relevant parameters were studied. Thus, the amount of enzyme to be deposited on the electrode was evaluated so that the linear response range of the methodology would fully cover the concentrations of glucose and ethanol expected in human sweat. It was found that 10 U of GOx mixed with the PdNCs (i.e., the modification of the WE of a 1WE-SPE with 6 μL of a mix containing 4 μg mL$^{-1}$ of PdNCs and 1667 U mL$^{-1}$ of GOx), were adequate for determining glucose in sweat, which is found in a variable concentration (usually between 0.0018 and 0.18 mg mL$^{-1}$ in diabetic patients) [40], although Karpova et al. [41] mention that the width of the interval makes it impossible to define a clear threshold for differentiating hypo from hyperglycemia. In the case of ethanol, the concentration found in sweat depends entirely on the amount of alcohol ingested, since the concentration present naturally is very low (less than 1 μg mL$^{-1}$). As the alcohol content in sweat can be correlated with that of blood (being approximately 15% higher) it is possible to establish a legal limit for driving of about 0.6 mg mL$^{-1}$ [39]. Since this concentration is higher than that of glucose, it was decided to deposit a lower amount of enzyme activity (only 0.5 U of AOx along with the PdNCs, that is, 1WE-SPE modification with 6 μL of a mix containing 4 μg mL$^{-1}$ of PdNCs and 83 U mL$^{-1}$ of AOx) to adjust to the linear range. On the other hand, the effect of the measurement temperature was evaluated (Figure S2A,B), showing a notable improvement when working at 37 °C compared to RT (which is expected considering that the optimum working temperatures for both enzymes are 35 °C for GOx [42] and 37 °C for AOx) [43]. In the case of glucose measurements, the sensitivity increase was from $290 \pm 20$ to $510 \pm 20$ μA cm$^{-2}$ mg$^{-1}$ mL (a 1.8-fold increase), while for ethanol the sensitivity increased from $67 \pm 4$ to $82 \pm 4$ μA cm$^{-2}$ mg$^{-1}$ mL, resulting in a 1.2-fold increase ($p < 0.05$). Moreover, the fit to the linear model, measured by $R^2$, also improved, especially in the case of glucose (from 0.984 to 0.993 for glucose and from 0.990 to 0.992 for ethanol). Although the use of the oven allowed us to improve the sensitivity of the methodology, it is also possible to measure at RT. Also, using a potentiostat combined with a heater would favor decentralized measurements [44].

In Figure 2A, linear sweep voltammograms were recorded at 100 mV s$^{-1}$ in 10 mM PBS on cells with the WE enzymatically modified, with GOx or AOx. The signal for the ORR was very similar to that obtained on the bare electrode. When double modification, with PdNCs and enzymes (GOx or AOx) using optimized concentrations was carried out, the catalytical effect was clearly observed, being very similar for both enzymes and, also, for the voltammogram recorded on the bare electrode. For the sake of comparison, voltammograms were also recorded in oxygen-free solutions, achieved by bubbling $N_2$ for 10 min and performing the measurements in a $N_2$ atmosphere. The results are like those previously observed in Figure 1C, with a large decrease in current density observed when $O_2$ is removed from the solution. However, since a small concentration of oxygen remains after bubbling, a clear but slight difference could be observed when electrodes were modified with PdNCs, with the catalytical effect seen either with or without enzymes (Figure 1C, dotted lines).

The scan rate employed, 100 mV s$^{-1}$, implies that recording a linear sweep voltammogram from 0 to −1 V takes 10 s. If we consider that ORR starts at ≈ −0.2 V with nanomodified WE or ≈ −0.4 V without PdNCs, this time is reduced to 2 or 4 s. However, enzymatic reaction starts just when the substrate drop (containing either glucose or ethanol) is added. By the time the initial potential is applied and scanned, arriving at the value required for ORR, a decrease in the oxygen concentration on the surface of the electrode has occurred and can be electrocatalytically measured. To see the difference when a very low scan rate is employed, for the system GOx/glucose, LSVs were recorded at only 1 mV s$^{-1}$ in 10 mM PBS (Figure 2B), taking 1000 s to scan the potential from 0 to −1 V. The results obtained are like those observed in Figure 2A but with lower current densities and lower electrocatalytical effect. The SPEs with the WE modified with PdNCs (with or without GOx) exhibit the ORR at a lower potential than that observed for unmodified electrodes. When glucose is added at a concentration of 0.25 mg mL$^{-1}$, ORR becomes negligible. At this very low scan rate, requiring 5 min to reach −0.3 V, the potential at which approximately ORR starts, important enzymatic oxygen consumption happens. Moreover, an electrochemical process, most likely due to HER (hydrogen



21922659, 2026, 16, Downloaded from https://advanced.onlinelibrary.wiley.com/doi/10.1002/adhm.202504371 by Spanish Cochrane National Provision (Ministerio de Sanidad), Wiley Online Library on [27/04/2026]. See the Terms and Conditions (https://onlinelibrary.wiley.com/terms-and-conditions) on Wiley Online Library for rules of use; OA articles are governed by the applicable Creative Commons License

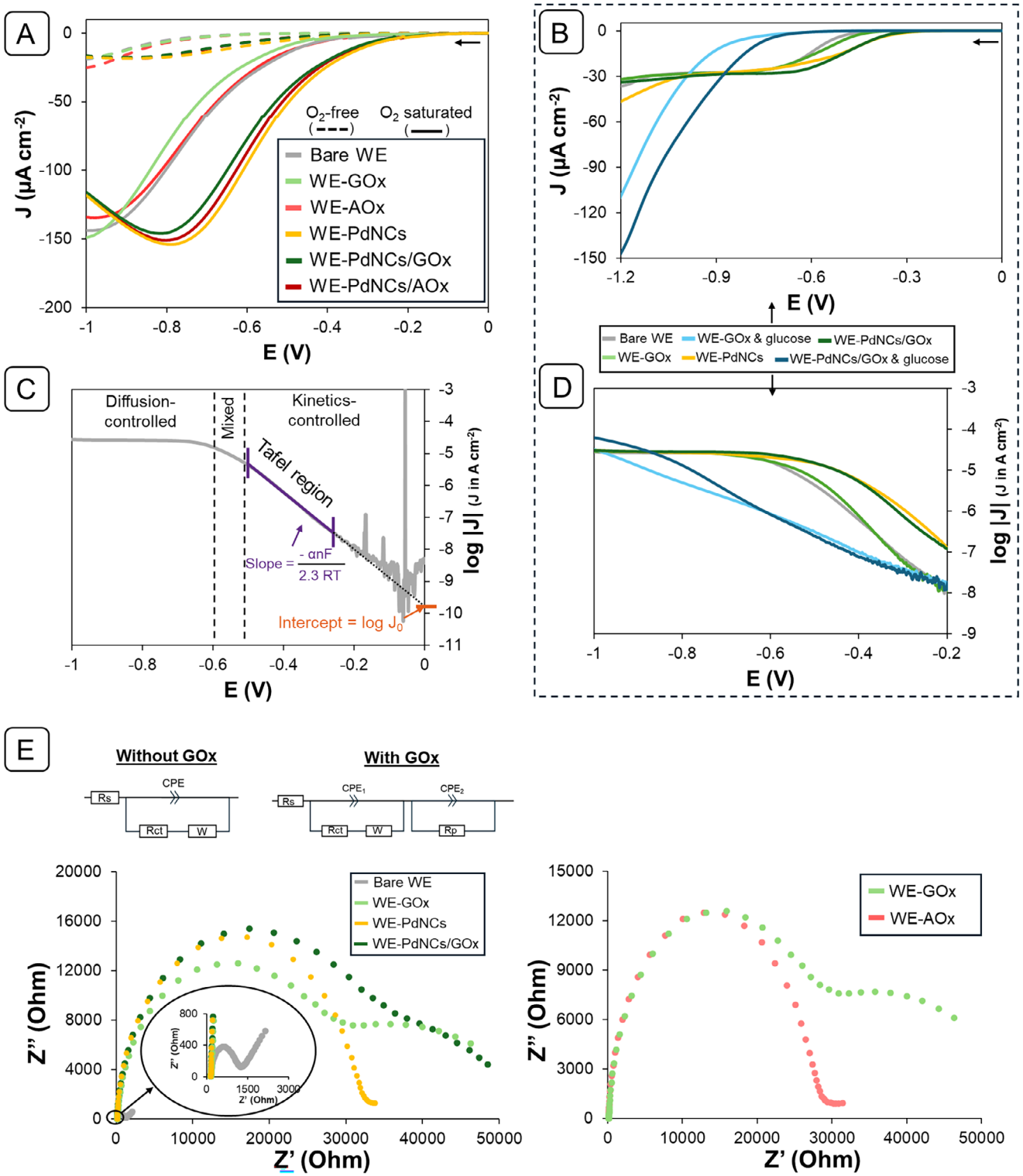



**FIGURE 2** | (A) LSVs recorded in either oxygen-free or oxygen-saturated PBS at a scan rate of 100 mV $s^{-1}$ on cells with bare WE, and WE biomodified with either GOx or AOx, or nanomodified with PdNCs, or bionanomodified with PdNCs /enzyme. (B) LSVs recorded in oxygen-saturated PBS at a scan rate of 1 mV $s^{-1}$ on cells with bare WE, and WE nanomodified with PdNCs, biomodified with GOx, or bionanomodified with PdNCs and GOx. Those modified with GOx were measured in the presence and absence of glucose (0.25 mg $mL^{-1}$). (C) Tafel plot for the LSV recorded at 1 mV $s^{-1}$ in 10 mM PBS pH 7.0 showing the different regions and the meaning of the slope and intercept of the line obtained in the Tafel region. (D) Tafel plots for the LSVs shown in (B). (E) EIS studies: (left) Nyquist plots for bare WE, and WE nanomodified with PdNCs, biomodified with GOx, or bionanomodified with PdNCs and GOx; (right), Nyquist plots for SPEs modified with AOx and GOx. The standard Randles equivalent circuit and its adapted version for GOx modified electrodes are also shown at the top.



21922659, 2026, 16, Downloaded from https://advanced.onlinelibrary.wiley.com/doi/10.1002/adhm.202504371 by Spanish Cochrane National Provision (Ministerio de Sanidad), Wiley Online Library on [27/04/2026]. See the Terms and Conditions (https://onlinelibrary.wiley.com/terms-and-conditions) on Wiley Online Library for rules of use; OA articles are governed by the applicable Creative Commons License

evolution reaction) is observed, which in the PdNCs-modified SPEs begins at a lower potential.

By plotting the corresponding Tafel plots (log J vs. E), kinetic parameters of interest, that is, exchange density of current ($J_o$) and charge transfer coefficient ($\alpha$), could be obtained for the diverse situations. Figure 2C explains the different regions, being the Tafel region this of relevance, since the linear relationship between log J and E, allows extracting these kinetic parameters from the intercept and the slope of the corresponding linear regression equations. Figure 2D shows the Tafel plots for the experimental results (LSVs recorded at 1 mV $s^{-1}$), performing the linear regression between −0.25 and −0.5 V or between −0.2 and −0.4 V for unmodified or for PdNC-modified SPEs, respectively. In this way, values for the Tafel slope (inverse of the slope obtained in the Tafel region) of −115 ± 3 and −122 ± 2 mV $dec^{-1}$ are obtained for unmodified and modified with PdNCs SPEs, respectively. When modification with GOx is made, the slope is slightly lower in both cases, −104 ± 6 and −117 ± 5 mV $dec^{-1}$ for those electrodes without or with PdNCs. These values are consistent with those reported in the literature [45], with −120 mV $dec^{-1}$ being the theoretical slope for ORR when the process is limited by a one-electron charge transfer step. This implies a charge transfer coefficient close to 0.5 (0.51 ± 0.1, 0.49 ± 0.1, 0.56 ± 0.2, and 0.52 ± 0.1, respectively), obtained from the slope values ($\alpha = -2.303\ RT/nFm$, where R is the universal gas constant (in J $mol^{-1}$ $K^{-1}$), T is the absolute temperature (in K), n is the number of electrons transferred in the rate-determining step (1 electron in this case), F is the Faraday constant (in C $mol^{-1}$) and $m$ the slope obtained from the Tafel plot (in V $dec^{-1}$) [45]. It should be noted that at higher potentials, the process is no longer limited by reaction kinetics and after a mixed region, it becomes limited by diffusion. In contrast, no different regions were observed in the Tafel plots after adding 0.25 mg $mL^{-1}$ of glucose in 10 mM PBS, but a continuous line with Tafel slopes of −220 ± 30 mV $dec^{-1}$ and −240 ± 20 mV $dec^{-1}$, for SPEs modified with GOx and with PdNCs and GOx, respectively.

In adition, EIS was used to characterize the surface of the enzymatic nanobiosensors. Figure 2E shows the Nyquist graphs (Z″ vs. Z′) obtained for unmodified SPEs and those biomodified with enzymes GOx or AOx, or nanomodified with PdNCs, as well as those bionanomodified. Figure 2E also shows the Randles equivalent circuit, and also the model circuit proposed when GOx is used. A large difference in the charge transfer resistance ($R_{ct}$) between the bare SPE (1620 ± 50 Ω) and the SPEs with the different modifications can be observed. When using nanomodification with PdNCs, it increases to 37 ± 2 kΩ. This could be due to the fact that, unlike metal nanoparticles, metal nanoclusters are not usually good conductors, and they are covered by an organic molecule (dihydrolipoic acid) that could reduce their conductivity [46]. Furthermore, when SPEs are modified with GOx, the presence of two semicircles indicates different charge transfer resistances. This can be observed on previous EIS studies with paper-based electrodes modified with a cocktail of enzymes containing GOx [47], and could be due to the formation of different phases in the protein layer ($R_p$), which, as other authors have reported [48], is most likely due to the packing of proteins on the electrode. Moreover, the difference between SPEs modified only with GOx and those combining PdNCs and GOx is significantly lower, 27± 1 kΩ vs. 34 ± 2 kΩ for $R_{ct}$, being the same for $R_p$, 16 ± 2 kΩ. To see if this happens with the other enzyme employed, the SPEs modified with AOx were compared with those modified with GOx. As seen in Figure 2E (right) the modification with AOx only present $R_{ct}$, following the Randles equivalent circuit, with a slightly higher value, 28 ± 3 kΩ than that found for GOx. Regarding the Warburg impedance (W) that accounts for mass transport (diffusion) of reactants, is only clearly observed as a ≈ 45° line on the Nyquist plot for the bare electrode, being masked in the rest of the cases.

### 3.3 | Analytical Characteristics of Single Nanobiosensors

Once optimized and characterized, a calibration curve was performed between 0.005 and 1 mg $mL^{-1}$ of glucose to know the analytical characteristics of the methodology (Figure 3A). It was found a linear range between 0.005 and 0.25 mg $mL^{-1}$ with a sensitivity of 395 ± 13 μA $cm^{-2}$ $mg^{-1}$ mL and a good fit to a straight line ($R^2$ = 0.994). Additionally, to evaluate the inter-sensor precision, cyclic voltammograms were recorded with seven sensors in 0.1 mg $mL^{-1}$ glucose solutions (Figure 3B), obtaining a value of density of cathodic current (measured at −0.55 V) of −91 ± 4 μA $cm^{-2}$ (RSD of 4.5%). For ethanol, a calibration in the range comprised between 0.05 and 10 mg $mL^{-1}$ was performed (Figure 3C), with a linear range covering up to 2.5 mg $mL^{-1}$, fitting well to a straight line ($R^2$ = 0.991), with a sensitivity of 48 ± 2 μA $cm^{-2}$ $mg^{-1}$ mL. Figure 3D shows the cyclic voltammograms obtained for seven ethanol sensors, for an ethanol concentration of 1 mg $mL^{-1}$, yielding a current density (measured also at −0.55 V) of −97 ± 3 μA $cm^{-2}$ (RSD of 2.7%).

### 3.4 | Multiplexed Sensor for Simultaneous Measurement of Glucose and Ethanol

Once it was confirmed, using SPE cell cards with a single WE, that the concentration of both glucose and ethanol can be determined using oxidase enzymes deposited along with the PdNCs, both sensors were integrated into a single platform using a 2WE-SPE as transducer to perform the simultaneous measurements of both substrates. A spatial separation approach has been chosen for the different analytes, since the same detection (ORR electrocatalysis of PdNCs) was employed. If both enzymes were in the same working electrode, total analysis (without differentiation between glucose or ethanol) could be made, obtaining just qualitative information. In this case, both WEs of these electrochemical cells, that share auxiliary and reference electrodes, were modified (Figure 4A), one with the mix containing PdNCs and GOx, and the other with this containing PdNCs and AOx. Thus, the miniaturized nanobioplatform employed for multianalyte determination uses the same nanocatalyst, that gives sensitivity, and two different biocatalysts to provide selectivity. These WEs were significantly smaller in area (2.3 $mm^2$ compared to 7.1 $mm^2$ of the WE in the single WE cell), so it was necessary to reduce the volume deposited to prevent the drops containing the modifiers from merging. Thus, it was reduced from 6 to only 1.5 μL, that was the volume deposited over each WE. Therefore, the concentrations of PdNCs and enzymes in the mixture were proportionally increased to have the same amount per $cm^2$ (i.e., number of μmols of substrate converted or product generated



21922659, 2026, 16, Downloaded from https://advanced.onlinelibrary.wiley.com/doi/10.1002/adhm.202504371 by Spanish Cochrane National Provision (Ministerio de Sanidad), Wiley Online Library on [27/04/2026]. See the Terms and Conditions (https://onlinelibrary.wiley.com/terms-and-conditions) on Wiley Online Library for rules of use; OA articles are governed by the applicable Creative Commons License

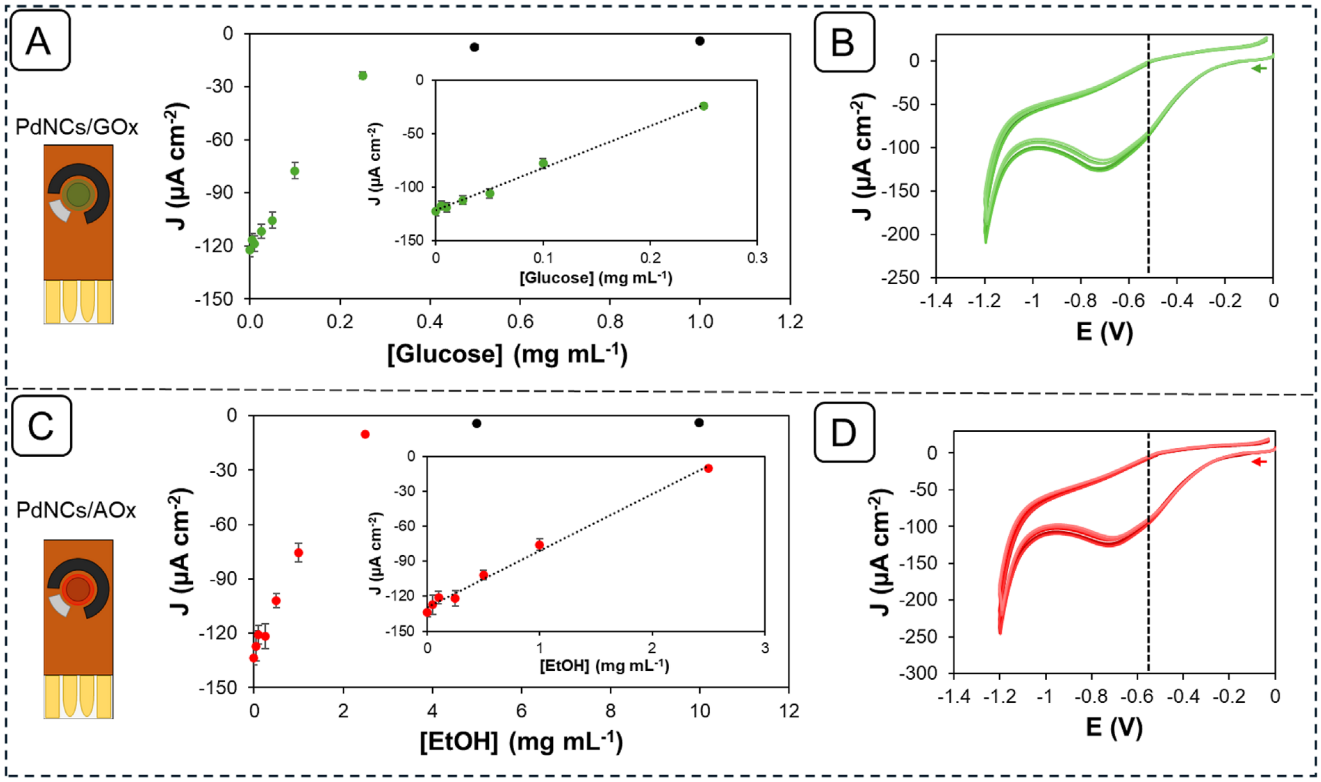



**FIGURE 3** | Calibration plots for glucose and ethanol obtained under optimized conditions using 1WE-SPE modified with PdNCs and GOx or AOx, respectively. (A,C) Current density obtained measured at −0.55 V for (A) glucose concentrations comprised between 0.005 and 1 mg $mL^{-1}$ and (C) ethanol concentrations comprised between 0.05 and 10 mg $mL^{-1}$ with insets for the corresponding linear ranges, using 10 mM PBS pH 7.0 as electrolyte. (B,D) Seven voltammograms recorded for (B) 0.1 mg $mL^{-1}$ glucose and (D) 1 mg $mL^{-1}$ ethanol solutions in PBS. Error bars show the SD of the measurements of 5 nanobiosensors.

under specific conditions). Thus, 1.5 μL of a solution containing 5.2 μg $mL^{-1}$ of PdNCs and either 2160 U $mL^{-1}$ of GOx (left WE) or 108 U $mL^{-1}$ of AOx (right WE) were deposited. Consequently, both electrodes are modified with 0.34 μg $cm^{-2}$ PdNCs, the one at the left with 141 U $cm^{-2}$ of GOx and the other at the right with 7 U $cm^{-2}$ of AOx.

From this moment, we worked with artificial sweat, to emulate the conditions in sweat samples. To prevent variations in the pH of the sweat (as well as in salt concentration) from significantly affecting the electrochemical measurements, it was decided that the PdNCs (and the corresponding oxidase enzyme) would be deposited using 100 mM PBS pH 7.0, so that this solution would buffer the changes in pH and salinity of the samples at the electrode-electrolyte interface.

Blank measurements were recorded for five 2WE-SPEs modified with PdNCs and enzymes. As can be observed in Figure 4B, there were no significant differences ($p > 0.05$) between the signals for both WEs with the average cathodic signal being −120 ± 9 μA $cm^{-2}$ for the GOx-modified and −115 ± 8 μA $cm^{-2}$ for the AOx-modified electrode, measured in an oven at 37 °C. Also, the effect of the presence of enzymes on the catalytic activity of PdNCs was tested (Figure 4C), which allows us to conclude that the enzymes do not block the active sites of PdNCs, since there is no change in the analytical signal. For this study, both WEs of the 2WE-SPEs were modified: i) only with PdNCs, ii) with GOx/PdNCs or iii) with AOx/PdNCs. As can been seen in this figure, when only artificial sweat was measured (without glucose nor ethanol), there were no significant differences whether PdNCs were deposited with or without enzymes. Moreover, there were no significant differences between the signals recorded with WE 1 or WE 2. However, when measuring artificial sweat containing either 0.25 mg $mL^{-1}$ of glucose or 2.5 mg $mL^{-1}$ of ethanol, the current density was only reduced in the WE that was modified with the corresponding enzyme, that is, decrease after adding glucose in the WE modified with GOx/PdNCs, and after adding ethanol in the WE modified with AOx/PdNCs. This demonstrates that oxygen in solution is reduced locally on the electrodes. The fact that electrochemical measurements are interfacial (electrode/electrolyte) favors multianalyte determinations avoiding crossed contamination, if measurement time is not delayed.

Therefore, to confirm that there were not interelectrode interferences, and the decrease in oxygen concentration due to the enzymatic reaction was localized on the WEs surface during the time of the measurement without diffusing from one electrode to the other, 2WE-SPEs were prepared modifying one WE with PdNCs/GOx and the other with PdNCs/AOx. Figure 4D depicts the signal obtained for artificial sweat solutions with different concentrations of glucose (green) and ethanol (red). The first thing to note is that there is no significant difference ($p$>0.05) between the signal for the WE containing GOx (−142 ± 8 μA $cm^{-2}$) and that containing AOx (−136 ± 9 μA $cm^{-2}$) when artificial sweat is measured, which indicates the good precision of the



21922659, 2026, 16, Downloaded from https://advanced.onlinelibrary.wiley.com/doi/10.1002/adhm.202504371 by Spanish Cochrane National Provision (Ministerio de Sanidad), Wiley Online Library on [27/04/2026]. See the Terms and Conditions (https://onlinelibrary.wiley.com/terms-and-conditions) on Wiley Online Library for rules of use; OA articles are governed by the applicable Creative Commons License

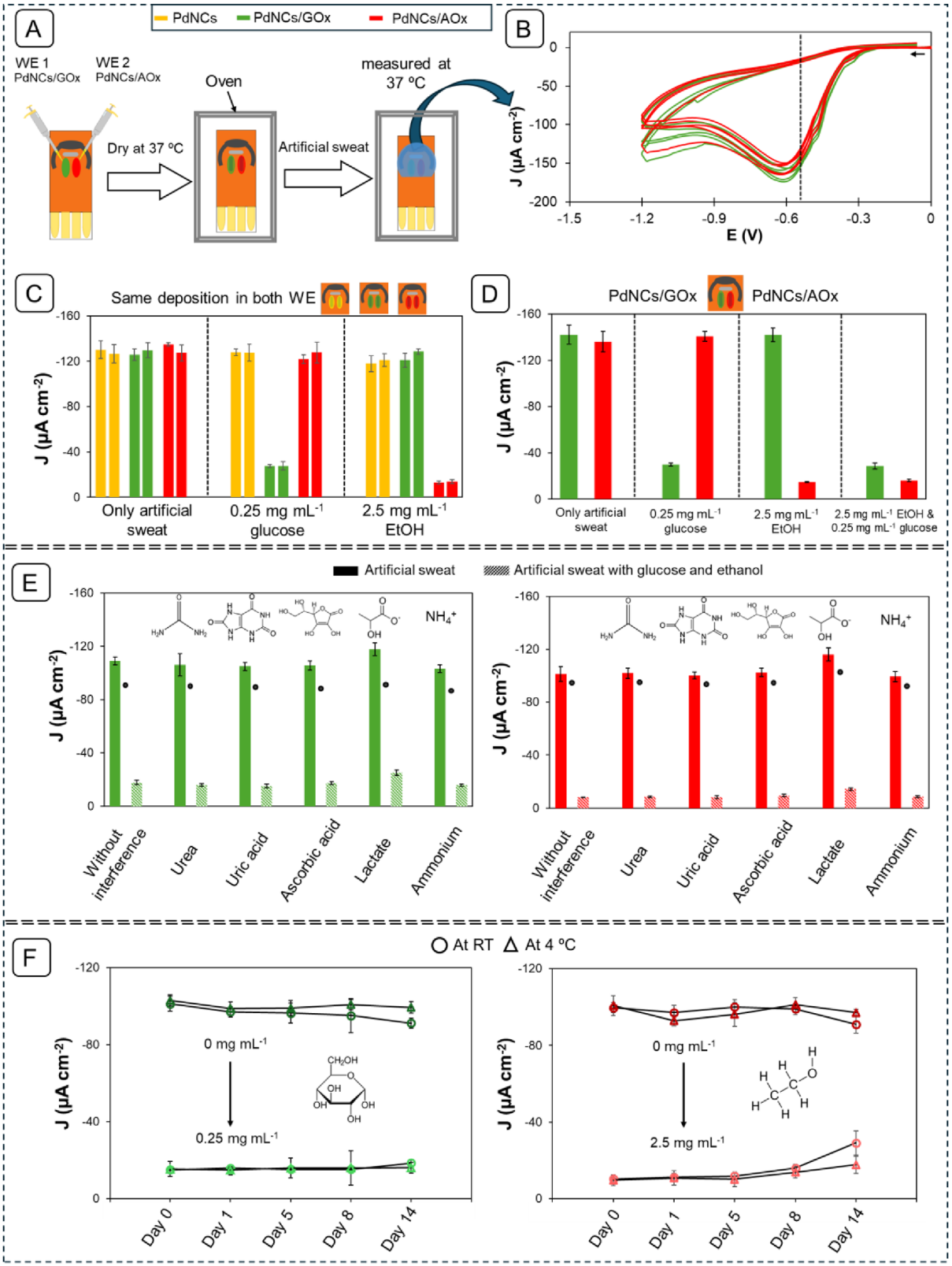



**FIGURE 4** | (A) Scheme of the independent modification of the two WEs. (B) A graph showing 10 voltammograms recorded on the 2 WEs of 5 electrochemical cells, in which each WE were modified either with PdNCs/GOx (green) or PdNCs/AOx (red). (C) Current densities obtained with 2WE-SPE where both WEs were modified with PdNCs (yellow), PdNCs/GOx (green) or PdNCs/AOx (red) in artificial sweat, or in a 0.25 mg $mL^{-1}$ of glucose or 2.5 mg $mL^{-1}$ of ethanol solution, both solved in artificial sweat. (D) Current densities obtained from voltammograms recorded with 2WE-SPEs where one WE was modified with PdNCs/GOx (green) and the other with PdNCs/AOx (red), in artificial sweat or in solutions containing 0.25 mg $mL^{-1}$ of glucose or 2.5 mg $mL^{-1}$ of ethanol, both prepared in artificial sweat solution. The last measurements were made in a solution containing both glucose (0.25 mg $mL^{-1}$) and ethanol (2.5 mg $mL^{-1}$) in artificial sweat. (E) Selectivity study. Current densities obtained from voltammograms recorded with 2WE-SPEs modified with PdNCs/GOx (left) and PdNCs/AOx (right). Measurements were performed in artificial sweat containing 0.25 mg $mL^{-1}$ of glucose and



21922659, 2026, 16, Downloaded from https://advanced.onlinelibrary.wiley.com/doi/10.1002/adhm.202504371 by Spanish Cochrane National Provision (Ministerio de Sanidad), Wiley Online Library on [27/04/2026]. See the Terms and Conditions (https://onlinelibrary.wiley.com/terms-and-conditions) on Wiley Online Library for rules of use; OA articles are governed by the applicable Creative Commons License

modified electrodes and the catalytical process. Furthermore, the results show that oxygen reduction occurs locally on the WEs, such that the signal of the WE containing GOx decreases only in the presence of glucose (−142 ± 8 vs. −30 ± 2 μA $cm^{-2}$; $p < 0.001$), and those modified with AOx are only affected by the presence of ethanol (−136 ± 9 vs. −16 ± 1 μA $cm^{-2}$; $p < 0.001$). As shown in Figure S3, when less than 3 min elapses from the addition of the solution containing 0.25 mg $mL^{-1}$ of substrate and the measurement, does not affect the signal at both WEs. For longer times a reduction in current density is observed at the AOx-modified electrode (in red), which may mean that a decrease in dissolved oxygen is occurring. Thus, depositing a different biocatalyst in a different WE (spatial separation of the biorecognition element) can be used to the simultaneous and selective determination of ethanol and glucose if the measurement takes less than 3 min, as in this case. CVs are recorded in 30 s, but since the measurement is performed on the forward scan, it is possible to record only linear sweep voltammograms (LSVs), which reduces the analysis time to the half (about 15 s).

It was found that when a solution containing both glucose and ethanol is measured, the signals decreased both in the GOx-modified WE (only due to the oxygen-mediated oxidation of glucose) and in the AOx-modified WE (only due to the oxygen-mediated oxidation of ethanol). No preconcentration step is required and no extra time is needed for the enzymatic reaction to run, so measurements can be performed in less than 1 min.

Once the effectiveness of the nanobiosensor had been demonstrated, the selectivity, that is, the effect of different interferents on the signal was evaluated. To do this, substances found in high concentrations in sweat were selected: urea, uric acid, ascorbic acid, lactate, and ammonium. In all cases, the highest physiological value within the normal range was selected, these being 720 mg $mL^{-1}$ for urea, 0.1 mg $mL^{-1}$ for uric acid, 1.76 mg $mL^{-1}$ for ascorbic acid, 3600 mg $mL^{-1}$ for lactate, and 136 mg $mL^{-1}$ for ammonium [49]. Figure 4E shows the difference in current density with (Iighter bars) and without (darker bars) adding substrates (0.25 mg $mL^{-1}$ of glucose and 2.5 mg $mL^{-1}$ of ethanol) to artificial sweat with or without interferents. The results are shown for the WE modified with PdNCs and GOx (left) and for the WE modified with PdNCs and AOx (right). The variations in the difference in current densities with and without interferents ranged from 96% to 102% for the WE modified with PdNCs/GOx, and from 99% to 109% in the case of the WE modified with PdNCs/AOx. The higher difference observed was for lactate in both cases, which could be due to an interaction between the carboxyl group of lactate, in high concentration, and PdNCs. Apart from these slight variations, it can be concluded that no significant differences were observed between undoped and doped artificial sweat for either glucose or ethanol.

Additionally, the stability of the nanobiosensor was evaluated over 14 days, both when stored at room temperature and at 4 °C. Figure 4F shows the current density recorded with SPEs with the WE modified with PdNCs/GOx (left) or PdNCs/AOx (right). When analyzing the results obtained, it can be seen that the baseline signal (attributable to PdNCs) does not vary significantly over time when storing the nanobiosensors either at RT or 4 °C, going from −101 ± 4 to −91 ± 3 μA $cm^{-2}$ at RT in the case of WE modified with PdNCs/GOx and from −100 ± 3 to −91 ± 5 μA $cm^{-2}$ for the WE modified with PdNCs/AOx. Thus, the signal obtained due to the PdNCs is only reduced by 10% compared to the initial signal when stored at RT and even less (< 3%) when stored at 4°C. For enzyme-modified SPEs, in the case of GOx, the difference is very slight when stored at RT (from −15 ± 1 to −19 ± 2 μA $cm^{-2}$), and no differences are observed when the sensors are stored at 4 °C. In the case of AOx, the differences are much more noticeable (−10 ± 1 vs. −30 ± 6 μA $cm^{-2}$) and can be observed after 8 days (−10 ± 1 vs. −16 ± 2 μA $cm^{-2}$) at RT. As with GOx, the enzyme is more stable at 4 °C, although significant differences are still apparent after 14 days (−10 ± 1 vs. −18 ± 2 μA $cm^{-2}$). We can therefore conclude that the nanobiosensor developed is very stable and can be stored for more than 5 days at RT without affecting bioelectrocatalysis. If longer storage is required, it can be done at 4 °C for, at least, 14 days, with only a slight reduction in the enzymatic activity of AOx. In any case, if commercialization is aimed, more thorough studies need to be made.

### 3.5 | Determination of Glucose and Ethanol in Sweat Samples

After demonstrating the possibility of performing a simultaneous determination of glucose and ethanol with the same platform and spatial separation of the biocatalytical elements (but sharing the same electrocatalyst), the method for sample collection was selected.

Direct measurement should be possible using a smartphone coupled with a minipotentiostat, since both sweat salinity and pH allow electrochemical measurements without the need for additional reagents. However, although electrodes were flexible (Figure 5A) and sampling is fast (membranes with ca. 5 μL of capacity), the modification with PdNCs, whose biotoxicity has not been tested, prevents from placing the modified electrodes directly on the skin, as shown in the image on the left. Nonetheless, no experiments were ever conducted directly on the skin, so Figure 5A remains purely as an example to illustrate the potential versatility of the developed nanobiosensor. To overcome this, electrodes could be placed without facing the skin (shown on the right), using an absorbent pad (Whatman chromatography paper) folded over the membrane adhered to the cell, so that the sweat could completely cover the 3 electrodes without coming PdNCs into contact with the skin. While this might be possible, for the

2.5 mg $mL^{-1}$ ethanol (lighter) or in artificial sweat without glucose nor ethanol (darker), and different interferents: 720 mg $mL^{-1}$ of urea, 0.1 mg $mL^{-1}$ of uric acid, 1.76 mg $mL^{-1}$ of ascorbic acid, 3600 mg $mL^{-1}$ of lactate, and 136 mg $mL^{-1}$ of ammonium. The black dot represents the difference between current densities obtained in the presence and absence of substrates. (F) Stability study. Current densities obtained from voltammograms recorded with 2WE-SPEs nanobiosensors that have been modified with PdNCs/GOx (left) and PdNCs/AOx (right) for artificial sweat solutions containing 0.25 mg $mL^{-1}$ of glucose and 2.5 mg $mL^{-1}$ ethanol (lighter) or not (darker) using nanobiosensors stored at RT (circles) or at 4°C (triangles). Error bars show the SD for measurements of 3 nanobiosensors.



21922659, 2026, 16, Downloaded from https://advanced.onlinelibrary.wiley.com/doi/10.1002/adhm.202504371 by Spanish Cochrane National Provision (Ministerio de Sanidad), Wiley Online Library on [27/04/2026]. See the Terms and Conditions (https://onlinelibrary.wiley.com/terms-and-conditions) on Wiley Online Library for rules of use; OA articles are governed by the applicable Creative Commons License

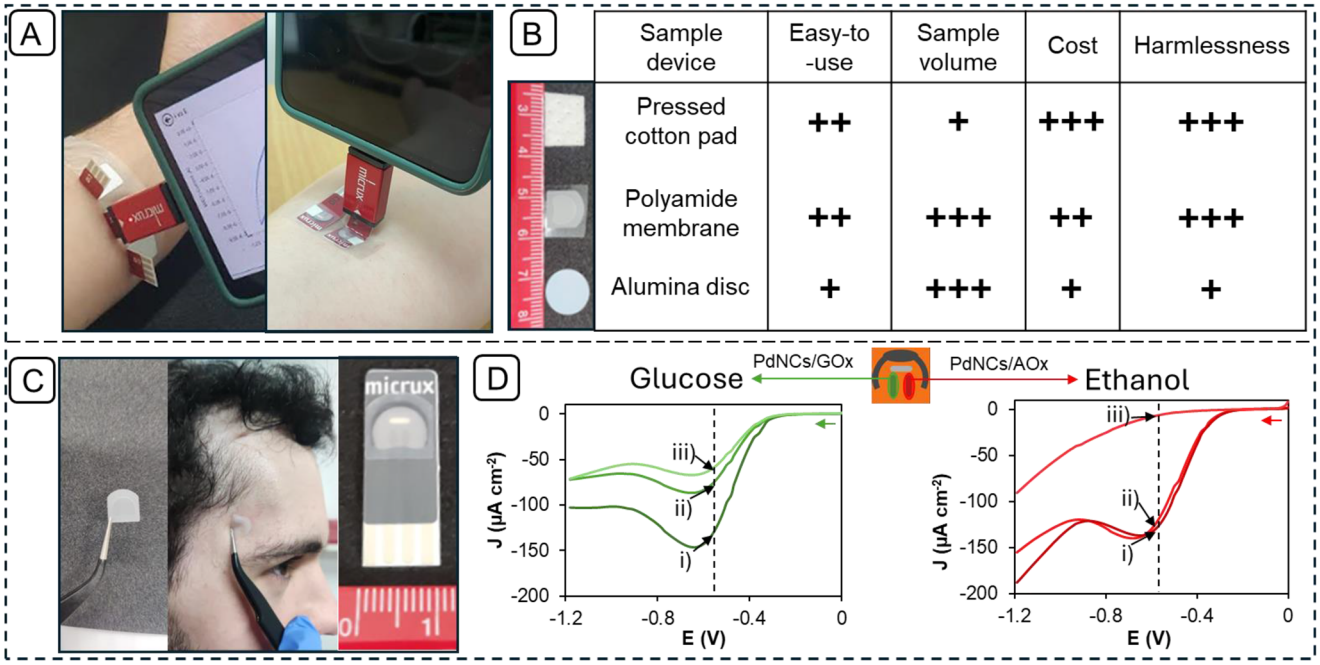



**FIGURE 5** | (A) Possibilities offered by the modified 2-WE SPEs for the creation of wearable devices using a USB type C-based potentiostat connected to a smartphone. The setup shows the direct placement of the SPE on the skin (left) and an alternative method using absorbent paper to avoid direct contact with the skin (right). (B) Comparison of the 3 materials used for sweat collection including a photograph of each one. (C) Pictures of a polyamide membrane held with a clamp (left), collection of sweat at the temple (center), and 2-WE SPE with the membrane sticked onto it (right). (D) LSVs recorded with the 2-WE SPE modified with PdNCs/GOx and PdNCs/AOx after each of the three rounds conducted: (i) drinking water/running, (ii) consuming a sugary drink/running and (iii) drinking an alcoholic beverage/running.

sake of simplicity, sweat was collected and then transferred to the cell for measurement. In this way, various alternatives were evaluated.

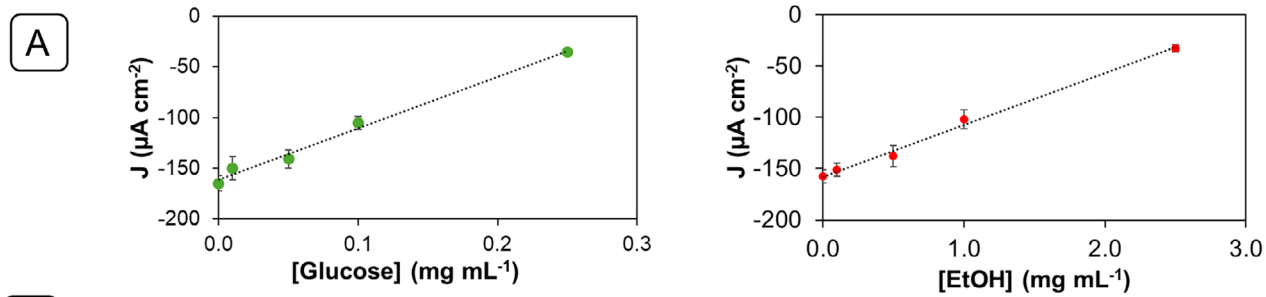
Polyamide membranes used in a previous work to reduce the volume necessary to cover all the electrodes of a screen-printed cell to less than 10 μL were tested [15]. Apart from this, other absorbent materials (pictures shown in Figure 5B) such as pressed cotton pads and nanoporous alumina discs were tested. Both cellulosic pads and polymeric membranes (flexible) pose no risk and are inert, being possible to use them on the skin. However, alumina discs are very fragile (only 60-μm thick) and rigid, and though, likely to break during the collection process (forming sharp edges). Figure 5B compares the characteristics of the collection materials. Regarding the cost, alumina discs are by far the most expensive (ca. 6 € per disc), followed by the membranes (less than 1 € per item). In this case, cotton pads were obtained by cutting a band-aid for the convenience (less than 0.25 € per item), but it would be possible to use pressed cotton to further reduce the price. Regarding the volume, in the case of the membranes, they take around 2 μL of sample, allowing for sample collection even if the amount of sweat secreted is low. In the case of the nanoporous alumina discs, they take approximately 25 μL, which is enough for measurements. However, they were discarded because of their fragility. Cotton absorbs a larger volume (around 70 μL for dimensions of 10 mm x 10 mm), but due to the fibrous nature, the sample could not be distributed as evenly as in the membranes, reducing the effectiveness of the measurements. This is because cotton is a vegetable textile fiber, so the distribution is not homogeneous as is the case of both membranes and alumina discs, whose pores are uniform in size. Therefore, cotton was also discarded. Polyamide membranes, finally chosen for collecting sweat samples, excel in precision in terms of collecting the same amount of volume, achieving an average of 2.2 ± 0.4 μL (for 10 replicates), being this low volume enough for the enzymatic reaction and further electrocatalytical measurement.

Figure 5C shows photographs of the membrane and of how it is used for the sample collection: after 30 min of physical exercise, sweat was taken from the temple holding the membrane with tweezers. This area of the body was selected because it is a highly sweaty and easily accessible area. Once the sweat was collected, the membrane was placed onto the screen-printed cell, and the membrane-cell platform was placed in the oven at 37 °C connected to the interface and/or potentiostat for immediate LSV measurement. Those obtained for glucose and ethanol in 2-WE SPEs nanobiomodified with PdNCs/GOx and PdNCs/AOx are shown in Figure 5D. They correspond to sweat collected from an individual after drinking 500 mL of water and running for 30 min, after drinking a sugary energy drink (500 mL, indicating a glucose content of 11 g per 100 mL) and running for 30 min, and after drinking a beer (250 mL, indicating a 5.5% of ethanol content) and running again for 30 min (always resting for 15 min to drink before starting physical activity).

Experimental results showed that there was a notable reduction in the analytical signal provided by the GOx-modified WE when a sugary beverage was consumed. The signal also slightly decreases after beer intake. In the case of the AOx-modified WE, the result is more noticeable, as there is not decrease after sugar consumption, but it drastically reduces upon alcohol consumption.



21922659, 2026, 16, Downloaded from https://advanced.onlinelibrary.wiley.com/doi/10.1002/adhm.202504371 by Spanish Cochrane National Provision (Ministerio de Sanidad), Wiley Online Library on [27/04/2026]. See the Terms and Conditions (https://onlinelibrary.wiley.com/terms-and-conditions) on Wiley Online Library for rules of use; OA articles are governed by the applicable Creative Commons License




B

| Day 1 | | Day 2 | | Day 3 | |
|---|---|---|---|---|---|
| Glucose (mg mL$^{-1}$) | Ethanol (mg mL$^{-1}$) | Glucose (mg mL$^{-1}$) | Ethanol (mg mL$^{-1}$) | Glucose (mg mL$^{-1}$) | Ethanol (mg mL$^{-1}$) |
| 0.06 ± 0.02 | <LOD | 0.07 ± 0.02 | <LOD | 0.05 ± 0.01 | <LOD |
| 0.09 ± 0.02 | <LOD | 0.09 ± 0.01 | <LOD | 0.08 ± 0.01 | <LOD |
| 0.10 ± 0.01 | 1.0 ± 0.2 | 0.11 ± 0.01 | 1.2 ± 0.3 | 0.10 ± 0.02 | 0.8 ± 0.2 |

| Subject 1 | | Subject 2 | |
|---|---|---|---|
| Glucose (mg mL$^{-1}$) | Ethanol (mg mL$^{-1}$) | Glucose (mg mL$^{-1}$) | Ethanol (mg mL$^{-1}$) |
| 0.06 ± 0.02 | <LOD | 0.04* | <LOD* |
| 0.10 ± 0.03 | <LOD | 0.08 ± 0.02 | <LOD |
| 0.09 ± 0.02 | 2.6 ± 0.1 | 0.08 ± 0.02 | 2.8 ± 0.1 |

(*) For a single SPE

C

| Subject 1 | | Subject 2 | |
|---|---|---|---|
| Sweat | Glucometer | Sweat | Glucometer |
| Glucose (mg mL$^{-1}$) | Glucose (mg dL$^{-1}$) | Glucose (mg mL$^{-1}$) | Glucose (mg dL$^{-1}$) |
| 0.06 ± 0.01 | 72 ± 4 | 0.08 ± 0.02** | 81 ± 3 |
| 0.09 ± 0.01 | 94 ± 3 | 0.10 ± 0.02* | 104 ± 5 |
| 0.08 ± 0.02 | 88 ± 5 | 0.10 ± 0.01 | 98 ± 3 |

| Subject 1 | | Subject 2 | |
|---|---|---|---|
| Sweat | Alcohol breath analyzer | Sweat | Alcohol breath analyzer |
| Ethanol (mg mL$^{-1}$) | Ethanol (g L$^{-1}$) | Ethanol (mg mL$^{-1}$) | Ethanol (g L$^{-1}$) |
| <LOD | 0.00 ± 0.01 | <LOD | 0.00 ± 0.01 |
| <LOD | 0.00 ± 0.01 | <LOD | 0.00 ± 0.01 |
| 0.9 ± 0.2 | 0.43 ± 0.06 | 0.7 ± 0.2 | 0.39 ± 0.04 |

(**) Mean ± SD for 3 SPEs

**FIGURE 6** | (A) Calibration curves obtained for 2WE-SPE modified with PdNCs/GOx and PdNCs/AOx for glucose (0.01–0.25 mg mL$^{-1}$) and ethanol (0.1–2.5 mg mL$^{-1}$) in artificial sweat. Error bars show the SD for measurements using 3 nanobiosensors. (B) Glucose and ethanol concentrations found in sweat samples of subjects after ingestion of water, a sugary energy drink, and an alcoholic beverage and further running after each ingestion. The experiment was performed on three different days for the same subject (left) and on the same day for two different subjects (right). (C) Simultaneous on-site (in a gym) determination of glucose and ethanol in sweat using the developed nanobiosensor, comparing glucose values with those found in blood using a glucometer and ethanol values with those of an alcohol breath analyzer. Measurements in figures A and B are shown as mean ± SD for 3 nanobiosensors and in C are shown for 4 nanobiosensors.

Once the experimental conditions and the sampling protocol were optimized, sample measurements were carried out. First, calibration curves for glucose and ethanol in artificial sweat using 2-WE SPEs with a polyamide membrane were carried out (Figure 6A). For glucose, a linear fit ($R^2$ = 0.990) was found in the range 0.01–0.25 mg mL$^{-1}$ with a sensitivity of 510 ± 30 μA cm$^{-2}$ mg$^{-1}$ mL, while for ethanol, the linear fit ($R^2$ = 0.994) was found in the range 0.1–2.5 mg mL$^{-1}$ with a sensitivity of 50 ± 2 μA cm$^{-2}$ mg$^{-1}$ mL. The detection limit found, calculated as the signal corresponding to three times the SD of the blank divided by slope, was 0.02 mg mL$^{-1}$ for glucose and 0.15 mg mL$^{-1}$ for ethanol.

Then, the nanobiosensor was applied to real sweat sample analysis of individuals that did physical exercise after consuming water, and sugary or alcoholic beverages. To take the sample, the polyamide membrane was placed on the temple of the individual



21922659, 2026, 16, Downloaded from https://advanced.onlinelibrary.wiley.com/doi/10.1002/adhm.202504371 by Spanish Cochrane National Provision (Ministerio de Sanidad), Wiley Online Library on [27/04/2026]. See the Terms and Conditions (https://onlinelibrary.wiley.com/terms-and-conditions) on Wiley Online Library for rules of use; OA articles are governed by the applicable Creative Commons License

and when saturated, it was placed onto the 2-WE SPE, covering all the three electrodes to take the measurement immediately at 37 °C. First, the sweat of the same individual was analyzed in three different days (Figure 6B, left). As can be observed for the 3 days, the sweat glucose level (after drinking water and running) increased significantly with the intake of a sugary energy drink (on average, 0.026 ± 0.007 mg $mL^{-1}$) and, in almost all the cases, it experienced a slight increase when an alcoholic beverage (beer) was ingested (0.016 ± 0.009 mg $mL^{-1}$). Since only 40 min have passed between the intake of the sugary drink and the glucose measurement, it is likely that the glucose level in the body continues to increase slightly over this time. In other studies, the maximum peak is reached 1 h after ingesting the food [50], so this could be in accordance with our results.

Regarding the concentration of ethanol, it remained below the detection limit in all cases where no alcoholic beverage was consumed. In this study, very small amounts of AOx were used, so the amount of enzyme could be increased to reduce the detection limits, if necessary. However, increasing the amount of AOx on the electrode would cause the ethanol signal to saturate faster, thus reducing the linear range. When consuming 250 mL of beer with 5.5% of alcohol content, a very significant increase in ethanol concentration in sweat was observed.

An independent study was conducted with two donor subjects. Figure 6B (right) shows that both individuals displayed analogous results regarding the fluctuation of glucose and ethanol. In this case, the amount of alcohol ingested was higher (250 mL of white wine with 13.5% of alcohol content) causing the ethanol concentration in sweat exceeding the linear range. This demonstrates that it is possible to simultaneously determine glucose and ethanol in human sweat using this small size nanobioplatform. If electrodes with a higher number of WEs are used, it should be possible to use the methodology to measure other oxidase substrates in sweat.

Finally, to evaluate how the nanobiosensor would perform when performing decentralized analyses, the protocol used in the study shown in Figure 6B was followed, but this time the measurements were carried out on-site in a gym. The exercise in this case consisted in running the same time but on an elliptical machine. Since a portable oven was not available, the measurements were taken at room temperature, so when the corresponding calibrations were performed, a reduction in sensitivity was observed. In particular, the sensitivity for glucose was reduced from 510 ± 30 to 320 ± 20 μA $cm^{-2}$ $mg^{-1}$ mL, while that for ethanol went from 50 ± 2 to 41 ± 3 μA $cm^{-2}$ $mg^{-1}$ mL. However, this reduction in sensitivity does not appear to have significantly affected the results obtained. These are shown in Figure 6C, where those obtained for the first two stages of the experiment (drinking water or a sugary drink) are very similar to those shown in Figure 6B, showing a notable increase in glucose concentration when ingesting the sugary drink. Ethanol values are below the detection limit in all cases. On the other hand, when drinking the alcoholic beverage, an increase in the concentration found in sweat was also observed. In contrast, in this case, not only was there no increase in glucose concentration after drinking the alcoholic beverage (like Figure 6B), but the concentration even decreased slightly. It has to be considered that there was a change in the conditions under which the aerobic exercise was performed, from running outdoors to running on an elliptical trainer in agym, which could have influenced the result.

Moreover, after completing the sweat measurements, blood glucose (using a glucometer) and ethanol (using an alcohol breath analyzer) measurements were taken. In the case of glucose, it can be observed that blood values fluctuate in a very similar way to how they vary in sweat, measured with the nanobiosensor developed. Likewise, the results obtained show that the concentration of glucose in sweat is only 8.6 ± 0.8% of that found in blood for subject #1 and, 9.5 ± 0.7% for subject #2. This is consistent with the literature, with reported concentrations of glucose in sweat usually 1–10% lower than in blood [51]. Similarly, the results using the breathalyzer also agree with the concentration of alcohol detected in sweat, responding only to the intake of alcoholic beverages. In particular, the concentration of ethanol in sweat was approximately twice that in blood, exactly 110 ± 20% and 70 ± 20% higher for subjects 1 and 2, respectively. These values are similar to those reported by other authors, since the concentration of ethanol in sweat is often higher than this present in blood. For example, Bhide et al. [33] report ethanol concentrations in sweat 40% higher than those found in blood.

These results show that the developed enzymatic nanobiosensor can be used in real world, allowing for decentralized in situ analysis, collecting sweat with polyamide membranes.

## 4 | Conclusions

This article has shown the development of multianalyte enzymatic nanobiosensors for sweat analysis, which have been evaluated in real world environment as a proof of concept. Initially, it has been proven that the electrocatalytical signal produced by PdNCs over ORR is affected by the localized oxygen concentration present on the WE surface, allowing the indirect measurement of substrates using their corresponding oxidase enzyme. This has been demonstrated for both glucose and ethanol, with both determinations being carried out simultaneously using SPE cells with 2 WEs, where selective deposition of PdNCs, with GOx on one electrode and AOx on the other one, was performed.

The use of membranes for sweat collection allows fast analysis without the need for external solutions or prior preparation, which greatly facilitates the implementation of miniaturized electrochemical devices. The simple and user-friendly methodology would allow individuals to perform self-analysis.

The developed methodology has quite low limits of detection for both glucose (0.02 mg $mL^{-1}$) and ethanol (0.15 mg $mL^{-1}$). When sweat samples were directly measured after running for 30 min, a noticeable increase in blood glucose was observed after consuming a sugary energy drink. It was also found that consumption of alcohol could be detected, even distinguishing between alcoholic beverages of different degrees.

The easy-to-use, flexible and disposable platforms can be operated with miniaturized bipotentiostats that are directly connected to smartphones, enabling decentralized and immediate measure-



21922659, 2026, 16, Downloaded from https://advanced.onlinelibrary.wiley.com/doi/10.1002/adhm.202504371 by Spanish Cochrane National Provision (Ministerio de Sanidad), Wiley Online Library on [27/04/2026]. See the Terms and Conditions (https://onlinelibrary.wiley.com/terms-and-conditions) on Wiley Online Library for rules of use; OA articles are governed by the applicable Creative Commons License

ments. This was verified by conducting a proof-of-concept test in a gym, where changes in glucose and ethanol concentrations in sweat measured using the enzyme nanobiosensor developed were simultaneously compared with those measured using a glucometer and an alcohol breath analyzer. The results obtained could be easily extrapolated to other oxidases, as they would all cause localized reduction of dissolved oxygen concentration on the electrodes, leading to a reduction in the PdNCs electrocatalytical signal. This would widen enormously the possible applications. Moreover, it would be advisable to continue developing it to allow measurements to move from decentralization, as the first step, to wearability.

### Author Contributions

A.R.-P.: Conceptualization: Supporting; Data curation: Lead; Formal analysis: Lead; Investigation: Lead; Methodology: Equal; Visualization: Lead; Writing – original draft: Lead. E.C.-R.: Conceptualization: Equal; Funding acquisition: Equal; Methodology: Equal; Project administration: Equal; Supervision: Equal; Writing – review & editing: Equal. B.F.: Funding acquisition: Equal; Supervision: Supporting; Writing – review & editing: Equal. M.T.F.-A.: Conceptualization: Lead; Funding acquisition: Equal; Methodology: Equal; Project administration: Equal; Supervision: Lead; Writing – review & editing: Equal

### Acknowledgements

This work was financially supported through projects PID2023-148375OB-I00 and PID2022-137319OB-C21 funded by MCIN/AEI/10.13039/501100011033/ FEDER, EU, and the Government of the Principality of Asturias through the Sekuens Agency, and EU through the FEDER Program (IDE/2024/000694). A. Rodríguez-Penedo thanks for the support of the "Severo Ochoa" Grant (PA-23-BP22-007) funded by the Government of the Principality of Asturias, Spain. Authors thank the support provided by the Mass Spectrometry Unit of the Servicios Científico-Técnicos and by the Servicio de Deportes, both from the University of Oviedo.

### Ethics Statement

The study was conducted in accordance with the recommendations of the Declaration of Helsinki. As commented in the Experimental Section, due to the small number of participants and the non-invasiveness of the collection protocol, it was not considered necessary to ask for approval to the Ethics Committee. At no point were measurements taken directly on the skin or using wearable formats. Nevertheless, all participants provided written informed consent prior to sample collection, shown in the Supporting Information. Data was fully anonymized to ensure participant confidentiality, in accordance with the Declaration of Helsinki on biomedical research involving human subjects.

### Conflicts of Interest

M.T.F-A is a co-founder of Micrux Technologies, a company engaged in the development of miniaturized electrodes and electrochemical/microfluidic equipment, and she remains a consultant and shareholder. She declares that this relationship did not influence the work reported in this paper. The other authors have no personal or financial conflicts of interest.

### Data Availability Statement

The dataset that supports this study is available in the Repository of the University of Oviedo via the following link http://dx.doi.org/10.17811/ruo_datasets.82310.

### References

1. E. R. Dorsey, B. Kluger, and C. H. Lipset, "The New Normal in Clinical Trials: Decentralized Studies," *Annals of Neurology* 88 (2020): 863–866, https://doi.org/10.1002/ana.25892.

2. P. Jain, A. M. Joshi, S. P. Mohanty, and L. R. Cenkeramaddi, "Non-Invasive Glucose Measurement Technologies: Recent Advancements and Future Challenges," *IEEE Access* 12 (2024): 61907–61936, https://doi.org/10.1109/ACCESS.2024.3389819.

3. G. C. Biswas, S. Choudhury, M. M. Rabbani, and J. Das, "A Review on Potential Electrochemical Point-of-Care Tests Targeting Pandemic Infectious Disease Detection: COVID-19 as a Reference," *Chemosensors* 10 (2022): 269, https://doi.org/10.3390/chemosensors10070269.

4. J. Wu, H. Liu, W. Chen, B. Ma, and H. Ju, "Device Integration of Electrochemical Biosensors," *Nature Reviews Bioengineering* 1 (2023): 346–360, https://doi.org/10.1038/s44222-023-00032-w.

5. E. H. Yoo and S. Y. Lee, "Glucose Biosensors: an Overview of Use in Clinical Practice," *Sensors* 10 (2010): 4558–4576, https://doi.org/10.3390/s100504558.

6. A. Altun, R. M. Apetrei, and P. Camurlu, "Reagentless Amperometric Glucose Biosensors: Ferrocene-Tethering and Copolymerization," *Journal of The Electrochemical Society* 167 (2020): 107507, https://doi.org/10.1149/1945-7111/ab9c81.

7. L. Lee, N. Loew, W. Tsugawa, K. Ikebukuro, and K. Sode, "Development of a Third-generation Glucose Sensor Based on the Open Circuit Potential for Continuous Glucose Monitoring," *Biosensors and Bioelectronics* 124-125 (2019): 216–223, https://doi.org/10.1016/j.bios.2018.09.099.

8. G. A. Naikoo, F. Arshad, I. U. Hassan, et al., "Trends in Bimetallic Nanomaterials and Methods for Fourth-Generation Glucose Sensors," *TrAC Trends in Analytical Chemistry* 162 (2023): 117042, https://doi.org/10.1016/j.trac.2023.117042.

9. E. C. Welch, J. M. Powell, T. B. Clevinger, A. E. Fairman, and A. Shukla, "Advances in Biosensors and Diagnostic Technologies Using Nanostructures and Nanomaterials," *Advanced Functional Materials* 31 (2021): 2104126, https://doi.org/10.1002/adfm.202104126.

10. P. Menero-Valdés, L. Álvarez, H. González-Iglesias, B. Fernández, and R. Pereiro, "Unveiling Compositional Images of Specific Proteins in Individual Cells by LA-ICP-MS: Labelling with Ruthenium Red and Metal Nanoclusters," *Analytica Chimica Acta* 1317 (2024): 342906, https://doi.org/10.1016/j.aca.2024.342906.

11. C. Toyos-Rodríguez, A. Adawy, F. J. García-Alonso, and A. de la Escosura-Muniz, "Enhancing the Electrocatalytic Activity of Palladium Nanocluster Tags by Selective Introduction of Gold Atoms: Application for a Wound Infection Biomarker Detection," *Biosensors and Bioelectronics* 200 (2022): 113926, https://doi.org/10.1016/j.bios.2021.113926.

12. X. L. Guevel, O. Tagit, C. E. Rodríguez, V. Trouillet, M. P. Leal, and N. Hildebrandt, "Ligand Effect on the Size, Valence State and Red/Near Infrared Photoluminescence of Bidentate Thiol Gold Nanoclusters," *Nanoscale* 6 (2014): 8091–8099, https://doi.org/10.1039/c4nr01130a.

13. A. Rodríguez-Penedo, E. Costa-Rama, R. Pereiro, B. Fernández, and M. T. Fernández-Abedul, "Immunoelectrochemical Assessment of human IgE in Non-Invasive Samples of Allergic Individuals Using PdNCs-Labelled Antibodies," *Microchimica Acta* 192 (2025): 237, https://doi.org/10.1007/s00604-025-07083-3.

14. S. Zhao, H. Zhang, S. D. House, R. Jin, J. C. Yang, and R. Jin, "Ultrasmall Palladium Nanoclusters as Effective Catalyst for Oxygen Reduction Reaction," *ChemElectroChem* 3 (2016): 1225–1229, https://doi.org/10.1002/celc.201600053.

15. A. Rodríguez-Penedo, P. Rioboó-Legaspi, A. González-López, et al., "Electrocatalytic Palladium Nanoclusters as Versatile Indicators of Bioassays: Rapid Electroanalytical Detection of SARS-CoV-2 by Reverse Transcription Loop-Mediated Isothermal Amplification," *Advanced Healthcare Materials* 12 (2023): 2202972, https://doi.org/10.1002/adhm.202202972.



21922659, 2026, 16, Downloaded from https://advanced.onlinelibrary.wiley.com/doi/10.1002/adhm.202504371 by Spanish Cochrane National Provision (Ministerio de Sanidad), Wiley Online Library on [27/04/2026]. See the Terms and Conditions (https://onlinelibrary.wiley.com/terms-and-conditions) on Wiley Online Library for rules of use; OA articles are governed by the applicable Creative Commons License

16. H. Li and G. Li, "Novel Palladium-Based Nanomaterials for Multifunctional ORR/OER/HER Electrocatalysis," *Journal of Materials Chemistry A* 11 (2023): 9383–9400, https://doi.org/10.1039/D3TA01059G.

17. G. N. Xing, D. Y. Wei, H. Zhang, Z. Q. Tian, and J. F. Li, "Pd-based Nanocatalysts for Oxygen Reduction Reaction: Preparation, Performance, and In-Situ Characterization," *Journal of Structural Chemistry* 42 (2023): 100021, https://doi.org/10.1016/j.cjsc.2023.100021.

18. P. Chen, Y. Peng, Y. Hao, Q. Huang, Y. N. Liu, and C. Deng, "A High Selective Disposable Biosensor Based on Screen-Printed Technique with Two Working Electrodes for Eliminating Interference Signals," *Sensors and Actuators B: Chemical* 183 (2013): 589–593, https://doi.org/10.1016/j.snb.2013.04.039.

19. C. Pothipor, J. Jakmunee, S. Bamrungsap, and K. Ounnunkad, "An Electrochemical Biosensor for Simultaneous Detection of Breast Cancer Clinically Related microRNAs Based on a Gold Nanoparticles/Graphene Quantum Dots/Graphene Oxide Film," *The Analyst* 146 (2021): 4000–4009, https://doi.org/10.1039/D1AN00436K.

20. W. Gao, S. Emaminejad, H. Y. Y. Nyein, et al., "Fully Integrated Wearable Sensor Arrays for Multiplexed In Situ Perspiration Analysis," *Nature* 529 (2016): 509–514, https://doi.org/10.1038/nature16521.

21. S. M. Khor, J. Choi, P. Won, and S. H. Ko, "Challenges and Strategies in Developing an Enzymatic Wearable Sweat Glucose Biosensor as a Practical Point-of-care Monitoring Tool for Type II Diabetes," *Nanomaterials* 12 (2022): 221, https://doi.org/10.3390/nano12020221.

22. F. Gao, C. Liu, L. Zhang, et al., "Wearable and Flexible Electrochemical Sensors for Sweat Analysis: A Review," *Microsystems & Nanoengineering* 9 (2023): 1, https://doi.org/10.1038/s41378-022-00443-6.

23. Y. Zhang, J. Liao, Z. Li, M. Hu, C. Bian, and S. Lin, "All Fabric and Flexible Wearable Sensors for Simultaneous Sweat Metabolite Detection and High-Efficiency Collection," *Talanta* 260 (2023): 124610, https://doi.org/10.1016/j.talanta.2023.124610.

24. M. Harun-Or-Rashid, M. N. Aktar, V. Preda, and N. Nasiri, "Advances in Electrochemical Sensors for Real-Time Glucose Monitoring," *Sensors & Diagnostics* 3 (2024): 893–913, https://doi.org/10.1039/D4SD00086B.

25. L. Oyagüez, F. Gómez-Peralta, S. Artola, et al., "Cost Analysis of freestyle Libre® 2 System in Type 2 Diabetes Mellitus Population," *Diabetes Therapy* 12 (2021): 2329–2342, https://doi.org/10.1007/s13300-021-01064-4.

26. D. G. Kulawiec, T. Zhou, J. L. Knopp, and J. G. Chase, "Continuous Glucose Monitoring to Measure Metabolic Impact and Recovery in Sub-Elite Endurance Athletes," *Biomedical Signal Processing and Control* 70 (2021): 103059, https://doi.org/10.1016/j.bspc.2021.103059.

27. M. Flockhart and F. J. Larsen, "Continuous Glucose Monitoring in Endurance Athletes: Interpretation and Relevance of Measurements for Improving Performance and Health," *Sports Medicine* 54 (2024): 247–255, https://doi.org/10.1007/s40279-023-01910-4.

28. R. Lin, F. Brown, S. James, J. Jones, and E. Ekinci, "Continuous Glucose Monitoring: A Review of the Evidence in Type 1 and 2 Diabetes Mellitus," *Diabetic Medicine* 38 (2021): 14528, https://doi.org/10.1111/dme.14528.

29. G. Brar, S. Carmody, A. Lumb, A. Shafik, C. Bright, and R. C. Andrews, "Practical Considerations for Continuous Glucose Monitoring in Elite Athletes with Type 1 Diabetes Mellitus: A Narrative Review," *The Journal of Physiology* 602 (2024): 2169–2177, https://doi.org/10.1113/JP285836.

30. C. Oba-Yamamoto, J. Takeuchi, A. Nakamura, et al., "Combination of Alcohol and Glucose Consumption as a Risk to Induce Reactive Hypoglycemia," *Journal of Diabetes Investigation* 12 (2021): 651–657, https://doi.org/10.1111/jdi.13375.

31. X. He, C. M. Rebholz, N. Daya, M. Lazo, and E. Selvin, "Alcohol Consumption and Incident Diabetes: The Atherosclerosis Risk in Communities (ARIC) Study," *Diabetologia* 62 (2019): 770–778, https://doi.org/10.1007/s00125-019-4833-1.

32. T. Kalaria, Y. L. Ko, and K. K. J. Issuree, "Literature Review: Drug and Alcohol-Induced Hypoglycaemia," *Journal of Laboratory and Precision Medicine* 6 (2021): 21, https://doi.org/10.21037/jlpm-21-16.

33. A. Bhide, S. Muthukumar, A. Saini, and S. Prasad, "Simultaneous Lancet-free Monitoring of Alcohol and Glucose from Low-Volumes of Perspired Human Sweat," *Scientific Reports* 8 (2018): 6507, https://doi.org/10.1038/s41598-018-24543-4.

34. Y. Shu, T. Su, Q. Lu, Z. Shang, Q. Xu, and X. Hu, "Highly Stretchable Wearable Electrochemical Sensor Based on Ni-Co MOF Nanosheet-Decorated Ag/rGO/PU fiber for Continuous Sweat Glucose Detection," *Analytical Chemistry* 93 (2021): 16222–16230, https://doi.org/10.1021/acs.analchem.1c04106.

35. M. Gamella, S. Campuzano, J. Manso, et al., "A Novel Non-Invasive Electrochemical Biosensing Device for In Situ Determination of the Alcohol Content in Blood by Monitoring Ethanol in Sweat," *Analytica Chimica Acta* 806 (2014): 1–7, https://doi.org/10.1016/j.aca.2013.09.020.

36. S. I. Suye, "Purification and Properties of Alcohol Oxidase from Candida Methanosorbosa M-2003," *Current Microbiology* 34 (1997): 374–377, https://doi.org/10.1007/s002849900198.

37. B. Sharma, S. Mandani, and T. K. Sarma, "Enzymes as Bionanoreactors: Glucose Oxidase for the Synthesis of Catalytic Au Nanoparticles and Au Nanoparticle–Polyaniline Nanocomposites," *Journal of Materials Chemistry B* 2 (2014): 4072–4079, https://doi.org/10.1039/C4TB00218K.

38. A. Lores-Padín, M. Cruz-Alonso, H. González-Iglesias, B. Fernández, and R. Pereiro, "Bimodal Determination of Immunoglobulin E by Fluorometry and ICP-MS by Using Platinum Nanoclusters as a Label in an Immunoassay," *Microchimica Acta* 186 (2019): 1–10, https://doi.org/10.1007/s00604-019-3868-9.

39. X. Xia, Y. Long, and J. Wang, "Glucose Oxidase-functionalized Fluorescent Gold Nanoclusters as Probes for Glucose," *Analytica Chimica Acta* 772 (2013): 81–86, https://doi.org/10.1016/j.aca.2013.02.025.

40. Y. Xiao, L. Hou, M. Wang, et al., "Noninvasive Glucose Monitoring Using Portable GOx-Based Biosensing System," *Analytica Chimica Acta* 1287 (2024): 342068, https://doi.org/10.1016/j.aca.2023.342068.

41. E. V. Karpova, E. V. Shcherbacheva, A. A. Galushin, D. V. Vokhmyanina, E. E. Karyakina, and A. A. Karyakin, "Noninvasive Diabetes Monitoring through Continuous Analysis of Sweat Using Flow-Through Glucose Biosensor," *Analytical Chemistry* 91 (2019): 3778–3783, https://doi.org/10.1021/acs.analchem.8b05928.

42. A. Rothberg, J. Weegar, R. Von Schalien, K. Fagervik, M. Rydström, and K. Lind, "Optimization of an Aspergillus niger Glucose Oxidase Production Process," *Bioprocess Engineering* 21 (1999): 307–312, https://doi.org/10.1007/PL00009075.

43. W. D. Murray, S. J. Duff, and P. H. Lanthier, "Induction and Stability of Alcohol Oxidase in the Methylotrophic Yeast Pichia Pastoris," *Applied Microbiology and Biotechnology* 32 (1989): 95–100, https://doi.org/10.1007/BF00164829.

44. P. Rioboó-Legaspi, A. González-López, J. F. Beltrán-Sánchez, et al., "Phenol Red as Electrochemical Indicator for Highly Sensitive Quantification of SARS-CoV-2 by Loop-Mediated Isothermal Amplification Detection," *Talanta* 266 (2024): 124963, https://doi.org/10.1016/j.talanta.2023.124963.

45. A. Holewinski and S. Linic, "Elementary Mechanisms in Electrocatalysis: Revisiting the ORR Tafel Slope," *Journal of The Electrochemical Society* 159 (2012): H864–H870, https://doi.org/10.1149/2.022211jes.

46. N. Qamhieh, "Investigation of the Electrical Properties of Metallic Nanoclusters," *The European Physical Journal D* 67 (2013): 37, https://doi.org/10.1140/epjd/e2012-30557-6.

47. O. Amor-Gutiérrez, E. C. Rama, and A. Costa-García, "Paper-Based Maskless Enzymatic Sensor for Glucose Determination Combining Ink and Wire Electrodes," *Biosensors and Bioelectronics* 93 (2017): 40–45, https://doi.org/10.1016/j.bios.2016.11.008.



21922659, 2026, 16, Downloaded from https://advanced.onlinelibrary.wiley.com/doi/10.1002/adhm.202504371 by Spanish Cochrane National Provision (Ministerio de Sanidad), Wiley Online Library on [27/04/2026]. See the Terms and Conditions (https://onlinelibrary.wiley.com/terms-and-conditions) on Wiley Online Library for rules of use; OA articles are governed by the applicable Creative Commons License

48. Q. Xie, C. Xiang, Y. Yuan, Y. Zhang, L. Nie, and S. Yao, "A Novel Dual-Impedance-Analysis EQCM System—Investigation of Bovine Serum Albumin Adsorption on Gold and Platinum Electrode Surfaces," *Journal of Colloid and Interface Science* 262 (2003): 107–115, https://doi.org/10.1016/S0021-9797(03)00196-6.

49. L. B. Baker and A. S. Wolfe, "Physiological Mechanisms Determining Eccrine Sweat Composition," *European Journal of Applied Physiology* 120 (2020): 719–752, https://doi.org/10.1007/s00421-020-04323-7.

50. H. J. Woerle, C. Meyer, J. M. Dostou, et al., "Pathways for Glucose Disposal after Meal Ingestion in Humans," *American Journal of Physiology-Endocrinology and Metabolism* 284 (2003): E716–E725, https://doi.org/10.1152/ajpendo.00365.2002.

51. P. H. Lin, S. C. Sheu, C. W. Chen, S. C. Huang, and B. R. Li, "Wearable Hydrogel Patch with Noninvasive, Electrochemical Glucose Sensor for Natural Sweat Detection," *Talanta* 241 (2022): 123187, https://doi.org/10.1016/j.talanta.2021.123187.

## Supporting Information

Additional supporting information can be found online in the Supporting Information section.

**Supporting-File**: adhm70923-sup-0001-SuppMat.docx.



21922659, 2026, 16, Downloaded from https://advanced.onlinelibrary.wiley.com/doi/10.1002/adhm.202504371 by Spanish Cochrane National Provision (Ministerio de Sanidad), Wiley Online Library on [27/04/2026]. See the Terms and Conditions (https://onlinelibrary.wiley.com/terms-and-conditions) on Wiley Online Library for rules of use; OA articles are governed by the applicable Creative Commons License